PHASE NOISE COMPENSATION FOR LONG-HAUL COHERENT OPTICAL COMMUNICATION SYSTEMS USING OFDM

by

© Jingwen Zhu

A Thesis submitted to the

School of Graduate Studies

in partial fulfillment of the requirements for the degree of

Master of Engineering

Department of Engineering and Applied Science

Memorial University of Newfoundland

October 2015

St. John's Newfoundland

ABSTRACT

Long-haul optical transmission systems employing coherent optical orthogonal frequency division multiplexing (CO-OFDM) are sensitive to laser phase noise. This causes a common phase rotation and inter-carrier interference. An effective method to compensate for the phase noise is to insert an RF-pilot tone in the middle of the OFDM signal. This RF-pilot is used to reverse the phase distortion at the receiver.

This thesis presents a detailed performance analysis of the RF-pilot phase noise compensation scheme in a simulated 64 Gbit/s CO-OFDM system. The effects of various parameters including laser linewidth, Mach-Zehnder modulator drive power, pilot-to-signal ratio, and fiber launch power are investigated. A comparison with the pilot-aided common phase error compensation method is provided to show the differences in the BER performance with respect to the required overhead.

ACKNOWLEDGEMENTS

First, I would like to express my gratitude to my supervisors: Dr. Venkatesan, Dr, O. Dobre, and Dr. Li. Thank you all for the help and support through my research and all the insightful conversations. Thank you for the opportunity to participate in the OmOptics Project.

I would like to thank all my colleagues, especially Lori and Yemi. Thanks for all the inspiring discussions and your help throughout my research and during my thesis writing time. It has been a pleasure working with you all.

Also, I would like to thank Atlantic Canada Opportunities Agency (ACOA), Research & Development Corporation of Newfoundland and Labrador (RDC), and Altera Canada for the support on the OmOptics Project and the inspiring workshop.

Finally, I would like to thank my family for their unconditional love and support and my friends for their help and encouragement throughout my time doing research.

Table of Contents

List of Figures

List of Symbols

A_{eff}	effective area of the optical fiber core
B_{ref}	reference bandwidth for noise
DGD_{MAX}	maximum budged differential group delay
f_c	center frequency of the optical carrier
N_A	number of optical amplifiers
N_c	number of subcarriers
N_p	number of pilot subcarriers
N_{TS}	average training symbol space
P_{ASE}	spontaneous emission noise power
P_S	transmitted signal power
R_s	symbol rate of the data
S_{OFDM}	baseband orthogonal frequency division multiplexing signal
T_g	guard time
β_2	group velocity dispersion parameter
ε_{TS}	training symbol overhead
η_2	non-linear refractive index
ϕ_1	transmitter carrier phase
ϕ_2	local oscillator carrier phase
Φ_{NL}	non-linear phase

ω_1	transmitter carrier frequency
ω_2	local oscillator carrier frequency
$\otimes$	convolution operation
A	signal amplitude
c	speed of light
D	dispersion parameter
h	channel response
p	polarization multiplexing of the signal
P_{OFDM}	electrical power of baseband orthogonal frequency division multiplexing signal
P_{RF}	electrical power of the RF-pilot
r	received signal
t	time
x	transmitted data
y	received data
z	transmission distance
α	attenuation coefficient
γ	nonlinear coefficient
Δf	OFDM subcarrier channel spacing
ω	optical angular frequency

List of Abbreviations

ACOA	Atlantic Canada Opportunities Agency
ADC	Analog-to-digital converter
ASE	amplified spontaneous emission
BER	bit error rate
BPF	band-pass filter
CD	chromatic dispersion
CO-OFDM	coherent optical OFDM
CP	cyclic prefix
CPE	common phase error
DAC	digital-to-analog converter
DDO-OFDM	direct-detection optical OFDM
DGD	differential group delay
DSP	digital signal processing
EDFA	erbium-doped fiber amplifier
FDE	frequency-domain equalizer
FEC	forward error corrections
FIR	finite impulse response
FWM	four-wave mixing
GVD	group velocity dispersion

ICI	inter-carrier interference
IMDD	intensity modulation and direct detection
IQ	in-phase and quadrature
ISI	inter-symbol interference
LO	local oscillator
LPF	low-pass filter
MZM	Mach-Zehnder modulator
OFDM	orthogonal frequency division multiplexing
OSNR	optical signal-to-noise ratio
PAPR	peak-to-average power ratio
PDM	polarization division multiplexing
PMD	polarization mode dispersion
PSK	phase-shift keying
PSR	pilot-to-signal ratio
QAM	quadrature amplitude modulation
RDC	Research & Development Corporation of Newfoundland and Labrador
SDM	space division multiplexing
SOP	state of polarization
SPM	self-phase modulation
SSMF	standard single mode fiber

TDE	time-domain equalizer
TS	training symbol
VPI	VPItransmissionMaker^{TM}OpticalSystems
WDM	wavelength division multiplexing
XPM	cross-phase modulation

Chapter 1 Introduction

1.1. Background of optical communication systems

1.1.1. Brief history of optical communications

Earliest optical communication systems can be traced back to 1790s [1]. C. Chappe invented the optical semaphore telegraph. In 1880s, almost a century later, A. Bell created an optical telephone system, Photophone, and it never became a commercial product [1]–[3]. The modern optical fiber communication was invented during the 1960s, with the invention of the lasers [4] and glass fibers [1]–[4]. During the same period of time, C. K. Kao and G. Hockham identified that optical fiber could be a suitable transmission medium if the attenuation could be reduced to a reasonable value (less than 20 dB per km) by achieving higher purity of glass fiber [1], [5]–[7]. At that time, the typical attenuation loss was as high as 1000 dB per km. In 1970, Corning Glass Works reached such low attenuation (lower than 20 dB per km) in single mode fiber operating at a wavelength of 633 nm [1]– [7]. This was made available commercially in 1975. The evolution of optical communication systems is usually categorized into four generations [3], [8]–[10], as described below.

The *first generation* of optical communication systems started in 1975 [6], [10], [11]. The systems operated on multimode fiber, near 800 nm with GaAs semiconductor lasers. However, the transmission performance was largely limited by the fiber loss, intermode

dispersion and intramode dispersion. The systems could reach a data rate of 45 Mbit/s and a transmission distance of 10 km without repeaters.

The *second generation* of optical communication systems was created in 1980s [12], [13]. The systems operated on single mode fiber, near 1300 nm with InGaAsP semiconductor lasers. Operating near 1300 nm wavelength, the fiber loss is as low as 1 dB per km. The transmission limitation caused by intermode dispersion is largely overcome by employing single mode fiber. The systems could reach a data rate as high as 1.7 Gbit/s and a transmission distance of 50 km without repeaters [11].

The *third generation* of optical communication systems was developed in late 1980s [8], [12], [14]. The systems operated on single mode fiber, near 1550 nm wavelength with InGaAsP semiconductor lasers [15]. Operating near 1550 nm wavelength, the fiber loss is as low as 0.2 dB per km. This fiber loss is less than that obtained when operating around 1300 nm wavelength, however, the chromatic dispersion is larger in the 1550 nm wavelength region. This problem can be solved by constraining laser spectrum to a single longitudinal mode or using dispersion-shifted fibers, whose core-and-cladding characteristic is adjusted in the way that the chromatic dispersion is minimum at the 1550 nm wavelength region. The systems could reach a data rate as high as 2.5 Gbit/s and a transmission distance of 100 km without repeaters [9].

The *fourth generation* of optical communication systems was developed in recent 30 years. Wavelength division multiplexing (WDM) technique [6], [9], [16], polarization

division multiplexing (PDM) [17], [18], and space division multiplexing (SDM) [19]–[21] are employed and hence the largely improved channel capacity. Optical amplifiers are also used to increase the transmission distance without repeaters. The systems could reach a data rate as high as 109 Tbit/s [21].

1.1.2. Introduction of coherent optical communications

In the 1980s, coherent optical communication systems had been intensively studied due to the high sensitivity of the coherent receivers [4], [9], [22]. The high sensitivity helped increase the transmission distance without using repeaters. However, with the employment of erbium-doped fiber amplifiers (EDFAs) in WDM systems, this development for coherent optical systems was delayed for almost 20 years, as explained later in this chapter. In 2005, a lot of interest in coherent optical communications was shown, following the demonstration of digital carrier phase estimation in these systems [23], [24]. This allows the use of various efficient modulation formats, such as M-ary phase-shift keying (PSK) and quadrature amplitude modulation (QAM). Before this, an optical phase-locked loop was a necessity [25]–[27]. Also, the phase information is preserved after detection, allowing electrical compensation methods for CD and PMD in digital domain. All factors contribute to the potential of higher transmission speed and higher spectrum efficiency of the coherent optical communication systems.

First stage of coherent optical communications: In 1970s, systems used intensity modulation of semiconductor lasers at the transmitter and used photodiode for direct

detection at the receiver side, known as intensity modulation and direct detection (IMDD) scheme. Compared with systems using IMDD scheme, coherent systems use an additional local oscillator (LO) source, enabling the restoration of full information on optical carriers, through in-phase and quadrature components of the complex amplitude of the optical electric field and the state of polarization (SOP) of the signal [28]. Modulation formats like QPSK or M-ary QAM can be applied, and thus including more information bits in one symbol [29].

However, the invention of EDFAs and their usage in WDM systems lessened the importance of the advantages brought by coherent systems.[28]. The system noise comes mainly from the accumulated amplified spontaneous emission (ASE) noise [22]. Complexity and cost for locking fast carrier phase shift and technical difficulties for implementing coherent receivers are all reasons for the fact that WDM systems with EDFAs were dominant instead of the coherent optical systems for a long period of time.

Revival of coherent optical communications: With the increase of the transmission capacity in WDM systems, the interest in coherent optical communications is once again high. The need to increase spectrum efficiency resulted in the use of multi-level modulation formats. In 2002, an experimental transmission using differential QPSK and optical in-phase and quadrature (IQ) modulation and the optical delay detection was reported [30]. Later in 2007, systems with a phase-diversity homodyne receiver could demodulate QPSK signal at a symbol rate of the 10-Gsymbol/s with the offline digital

signal processing [31].

One major advantage of coherent optical communications is that the spectrum efficiency is increased from 1 bit/s/Hz per polarization to M bit/s/Hz per polarization. One other advantage is the post-signal-processing function. The amplitude and the phase information are preserved even after the detection process, due to the fact that IQ modulation is a linear process. More powerful and efficient DSP solutions for CD, PMD, and phase noise compensation can be implemented after detection [32], [33].

1.2. Importance of phase noise compensation

In coherent optical communication systems, lasers are employed at both transmitter and receiver. The performance of systems using coherent detection techniques is affected by the phase noise introduced by the optical source, that is, the laser phase noise.

Laser phase noise is caused by instabilities in the light sources in optical communication systems, such as absorption, spontaneous emission, and stimulated emission. It is usually modeled as a Wiener process [34], [35]. Consequently, instead of a single frequency, the output of a laser has multiple frequencies, presenting a linewidth ranging from several hundreds of kHz to several MHz [36]–[38].

Phase noise is important for systems employing coherent detection as the information is carried by both the amplitude and phase of the data, instead of the energy of the data. Phase noise causes a rotation of the constellation of the received signal and impacts the

signal synchronization [39].

1.3. Motivation

From the discussion above, it is clear that coherent optical systems are suitable for long-haul transmission, and it is important to compensate for phase noise in coherent optical communication systems. This thesis focuses on compensating for phase noise for long-haul coherent optical systems using orthogonal frequency division multiplexing (OFDM), while coping with the challenges from the optical channel distortions.

This research work is a part of the OmOptics Project. OmOptics, Orthogonal Frequency Division Multiplexing Technology Development for Terabit Optical Transport Network, is a four-year project at Memorial University, funded through the Atlantic Innovation Fund by Atlantic Canada Opportunities Agency (ACOA), Research & Development Corporation of Newfoundland and Labrador (RDC), and industry collaborator Altera Canada. OFDM has been widely employed in wireless world. The aim of this project is to employ OFDM technology into optical communication systems, adapting to ultrahigh speed optical networks and creating new commercial products by developing, implementing, testing, and commercializing DSP algorithms.

1.4. Organization of the thesis

As has been discussed above, coherent optical communication systems have great potential in long-haul transmission and such systems face the problem of high sensitivity

to laser phase noise. This thesis focuses on a coherent optical OFDM system, simulates the channel distortions and laser phase noise, and implements and tests two DSP algorithms to combat these distortions. These algorithms can be implemented in WDM system to obtain ultrahigh data rates.

Here, a detailed study of digital signal processing (DSP) algorithms for compensating system impairments of coherent optical communication systems using orthogonal frequency division multiplexing (OFDM) has been provided. The systems in this work are assumed to have a bit rate of 64 Gbit/s and an optical fiber length of as long as 800 km. The work explores in detail the mitigation of optical channel impairments and compensation of phase noise.

Chapter 1 gives a quick introduction to the thesis organization. It briefly discusses the advances of coherent optical systems and how phase noise affects the performance of these systems. It also summarizes the history and recent development of the related research field.

Chapter 2 focuses on the major system impairments of the coherent optical OFDM (CO-OFDM) systems using standard single mode fiber (SSMF). It starts with the reasons to use SSMF and coherent detection instead of direct detection, and then moves onto the choice of systems using OFDM over single carrier systems. However, phase noise is a problematic factor in these systems. The reasons are explained. Also, optical channel impairments from SSMF are discussed as well: attenuation, chromatic dispersion (CD),

polarization mode dispersion (PMD), and fiber nonlinearities.

Chapter 3 uses MATLAB and VPItransmissionMaker as simulation tool to set up a specific CD-OFDM optical communication system using SSMF. This system is then used to demonstrate the degradation caused by different channel distortion, and corresponding compensation solutions are provided as comparison.

Chapter 4 focuses on phase noise and its compensation. It introduces RF-pilot phase noise compensation method and pilot-aided CPE method. The principles of both methods are explained and the important parameters are discussed in detail with simulation support. The performances of these methods are examined under long-haul transmission conditions.

Chapter 5 summarizes the entire thesis, highlights the contribution and discusses the potential future work.

Chapter 2 Major System Impairments in Long-haul CO-OFDM Communication Systems

This chapter starts with a general introduction to long-haul optical communication systems. Both coherent detection and direct detection schemes for such systems are introduced. Then the advantages and disadvantages for long-haul optical systems using single carriers or OFDM are discussed. And the conclusion that CO-OFDM is an appropriate choice for long-haul transmission is drawn.

A prominent problem for long-haul CO-OFDM systems is that they are highly sensitive to phase noise. The cause of phase noise and its impact on coherent optical systems are also studied.

Other impairments for long-haul CO-OFDM systems are mainly introduced by the optical fiber as the transmission channel: fiber attenuation, chromatic dispersion (CD), polarization mode dispersion (PMD), and fiber nonlinearities.

2.1. Long-haul optical communication systems

2.1.1. Comparison between single mode fiber and multi mode fiber

In Chapter 1, the use of multi mode fiber and single mode fiber was mentioned. In this thesis, all optical channels consist of multiple spans of standard single mode fiber (SSMF). The reasons are explained in this section.

Single mode fiber consists of a strand of glass fiber with a core diameter of 8.3 to 10 microns [11], [40]. The core has a relatively narrow diameter, allowing only one mode to transmit. The light travels toward the center of the core of the fiber with a single wavelength. The wavelength of the light usually operating on single mode fiber is 1310 nm or 1550 nm. It should be noticed that, in single mode fiber, two orthogonal polarization modes exist, that causes PMD. The constraint of the fiber core eliminates overlapping light pulses distortions, provides low attenuation and high transmission speed without compromising signal quality [8]. The transmission distance can be 50 times longer than using multimode fiber [41]. However, single mode fiber has the disadvantage of higher cost [1].

Multimode fiber consists of glass fibers with a core with diameter of 50 to 100 microns (typical diameters: 50, 62.5, and 100 micrometers) [6], [11]. The core is relatively large, allowing light travelling with different paths [4]. That is what multi mode refers to. The wavelength of the light usually operating on multi mode fiber is 850 nm or 1310 nm [40]. Compared with single mode fiber, multi mode fiber is more cost efficient. However, the multipath transmission distortion is prominent when the transmission distance is longer than around 900 meters. The received signal suffers from great distortion or even incomplete transmission.

This work focuses on long-haul transmission condition and uses simulation as research tool. As has been discussed before, single mode fiber is a more suitable candidate for

long-haul transmission. Therefore, all the optical fiber channels employed in this thesis consist of standard single mode fiber.

2.1.2. Optical OFDM communication systems

OFDM has been in existence since 1966 when Bell Labs filed a patent application for "Orthogonal Frequency Multiplex Data Transmission System" [42]. Since then, OFDM has evolved: using FFT instead of DFT to generate OFDM signal in 1969 [43]; adding cyclic prefix (CP) to combat inter symbol interference (ISI) in 1980 [44].

OFDM has been used for mobile communication in 1985 by Cimini of Bell Labs [45], [46]. Later on, it was used for radio broadcasting in Lassalle and Alard in 1987 [47]. It was not until 2001, OFDM became part of many wireless communication standards [48].

The various advantages of orthogonal frequency division multiplexing (OFDM), including its high spectral efficiency, robustness against multipath delay, and ease of channel and phase estimation, have resulted in OFDM being widely adopted in various wired and wireless communication standards since 2008 [20]. In recent years, advancements in the integrated circuit technology, developments in DSP algorithms, together with an increased demand for higher data rates across long fiber distances [42], have facilitated the transition of OFDM into the optical communications world communications in various areas, such as OFDM in optical wireless [49], OFDM in single mode fiber systems [50], and OFDM in multi mode fiber systems [51], [52].

IFFT and FFT are the key elements in the OFDM system transmitter and receiver respectively. The size of IFFT/FTT is essential to the design of a system using OFDM technique. The size of an IFFT/FTT is equal to the number of total subcarriers, which is usually a power of two. The typical size for IFFT/FTT is ranging from 128 to 1024 in practice. Larger IFFT/FTT size indicates lower data rate and data are less likely to suffer from ISI [42], [53], [54]. Also, the CP percentage is smaller, indicating smaller overhead. On the other hand, systems with smaller IFFT/FTT size are less complex to implement at both transmitter and receiver. Also, smaller FFT size reduces the sensitivity at the receiver if coherent detection is employed. It is important to consider all these factors when designing systems using OFDM.

CP is also an important parameter to consider when designing a system. CP is the replica of a certain percentage of an OFDM symbol. CP is then attached to the beginning of the OFDM symbol. At the receiver side, CP is deleted from the received data. The purpose of CP is to combat ISI and inter-carrier interference (ICI). It can also be used in symbol synchronization. Introducing CP increases the system redundancy, because CP is essential redundant information obtained from the data symbols. The percentage of CP should depend on the channel condition. For optical OFDM, the source for ISI is CD and PMD from the optical fiber channel. The required CP length (guard time) can be calculated using the equation below [55]:

$$\frac{c}{f_c^2} \cdot |D| \cdot N_c \cdot \Delta f + DGD_{MAX} \leq T_g, \quad (1)$$

where T_g represents the guard time, c is the speed of light, f_c is the center frequency of the optical carrier, D is the total amount of chromatic dispersion, with a dimension of s/m, N_c is the number of subcarriers, Δf is the OFDM subcarrier channel spacing, $DGD_{MAX}$is the maximum budgeted DGD. DGD can be approximated as 3.5 times the mean PMD in typical fiber specifications. Then, CP percentage can be calculated as guard time over OFDM symbol duration.

However, it is important to notice that in long-haul optical fiber transmission, ISI caused by CD and PMD cannot be completely eliminated by using CP with a reasonable percentage overhead. It is important to introduce more sophisticated methods to compensate for CD and PMD. This is elaborated in chapter 3.

Employing CO-OFDM has many advantages [56]: it is spectrum efficient by allowing overlapping; simply adding CP helps eliminate ISI and ICI; FFT is easy to implement and scale; compared with single carrier system, adaptive equalization can be used easily for channel equalization, lower sensitivity to sample timing offsets compared to single carrier system.

However, despite all the advantages, OFDM has its disadvantages and limitations, including high peak-to-average power ratio (PAPR) and high sensitivity to phase noise and frequency offset [57]. PAPR is a problem because of the fact that most components of the data spread around a wide range in the transmitter and receiver, which requires a large linear range for the amplifiers. Any distortion from the nonlinearities from the

amplifiers causes out-of-band power and in-band distortion.

Optical OFDM solutions can be classified into two broad groups based on the techniques used for detection at the receiver. These groups are direct-detection optical OFDM (DDO-OFDM) [58] and coherent optical OFDM (CO-OFDM) [59]. CO-OFDM, although featuring a higher degree of complexity at the transmitter and receiver sides than DDO-OFDM, has shown superior performance in terms of spectral efficiency and receiver sensitivity [57]. This makes CO-OFDM a suitable candidate for long-haul optical transmission. In Section 2.1.3, detection schemes for optical communication systems are discussed in detail.

2.1.3. Detection schemes for long-haul optical communication systems

In this section, two categories of detection schemes for optical communication systems are discussed: direct detection and coherent detection.

- **Direct detection**

For receivers using direct detection, the corresponding transmitters use intensity modulation, as was mentioned in Chapter 1. Those systems are known as IM/DD systems [1], [6], [54]. At the transmitter side, electrical current is transformed into photons. The output optical power has a linear relationship with the electrical input. They are modulated signals. This signal is usually a double side band signal, which can be filtered as single side band signal as needed.

At the receiver side, the received optical signal is detected by a photodiode, and its intensity is converted into electrical signal. To be more specific, the converted electrical signal has current variations proportional to the square of the incoming signal's optical field.

Figure 1 shows the two direct detection schemes for optical OFDM systems: with and without frequency gap between optical carrier and OFDM signal separately. In the former case, where there is a frequency gap between optical carrier and OFDM signal, the guard band B is enough for the subcarrier mixing. The guard band is known as the offset single side band and is equal to the bandwidth of the OFDM signal. This unwanted part can be easily filtered without compromising the quality of the OFDM signal. However, in this case, half the bandwidth is wasted, which is spectrum inefficient. Also, at the transmitter, ODFM signal needs to be up converted and at the receiver, OFDM signal needs to be down converted, which contributes to system complexity.

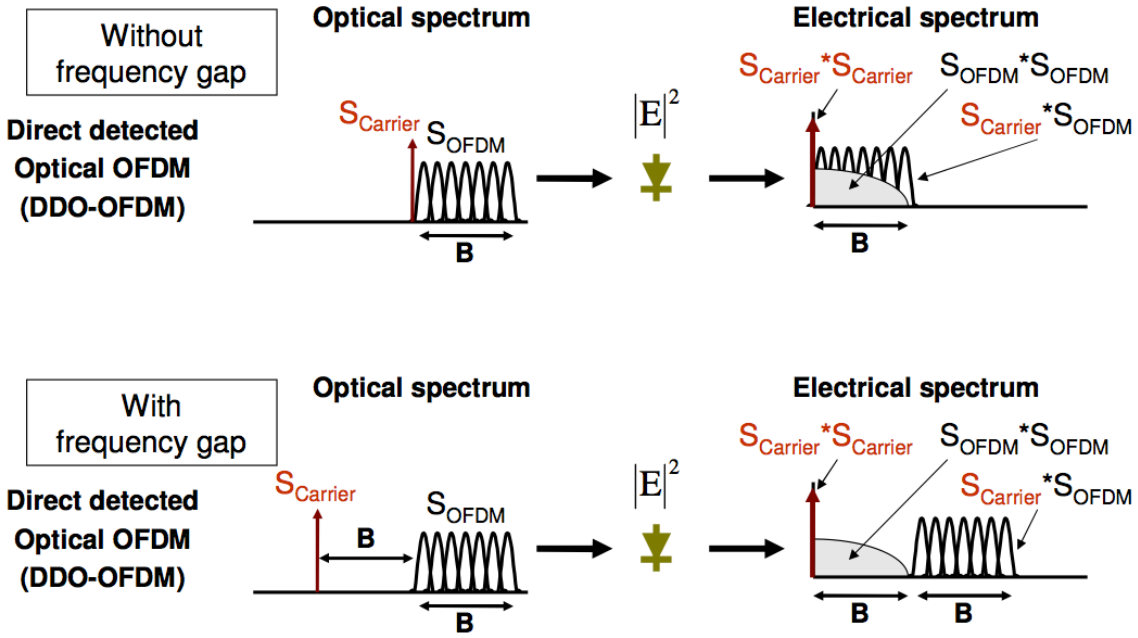

Figure 1 Direct detected optical OFDM (reproduced from [56]).

In the latter case, where there is no gap between optical carrier and OFDM signal, which is often called compatible side band method, the obvious advantage is that the full bandwidth is used for OFDM data transmission. However, the unwanted subcarrier mixing product needs to be eliminated by pre-compensation. Though this product is deterministic, the pre-compensation still contributes to the system complexity. Also, the system performance is limited to the effectiveness of the elimination of the unwanted mixing, since the mixing product also suffers from channel impairments.

More sophisticated methods for removal of the subcarrier mixing are proposed as well.

One of those methods proposed that a feedback loop is setup to help with the iterative decoding process [60]. This results in a better compensation performance, as well as further increased system complexity.

- **Coherent detection**

The principle of coherent detection is that the product of the electrical field of the received optical signal and the continuous wave local oscillator is the detected signal. The aim is to detect signals based on full electrical field. In this case, information can be modulated on both amplitude and phase, or in-phase (I) and quadrature (Q) component [9], [39].

Here, the detection procedure is explained for systems using the OFDM technique. At the transmitter side, the baseband electrical OFDM signal is modulated by IQ modulator to the carrier frequency. The transmitted signal can be modelled as [9]:

$$E(t) = exp\,(j\omega_1 t + \phi_1) \cdot S_{OFDM}(t), \tag{2}$$

where ω_1 is the carrier frequency, ϕ_1 is the carrier phase, and $S_{OFDM}(t)$ stands for the baseband OFDM signal. Assume the channel response is $h(t)$. Then the received optical signal $E'(t)$ can be modelled as:

$$E'(t) = ex\,p(j\omega_1 t + \phi_1) \cdot S_{OFDM}(t) \otimes h(t), \tag{3}$$

where $\otimes$ represents convolution operation. Considering the local oscillator has a carrier frequency of ω_2 and a carrier phase of ϕ_2, after the coherent detection, the detected RF

OFDM signal can be expressed as:

$$r(t) = exp\,(j(\omega_2 - \omega_1)t + (\phi_2 - \phi_1)) \cdot S_{OFDM}(t) \otimes h(t), \qquad (4)$$

After the channel, the received optical signal is then mixed with a local oscillator. Figure 2 shows coherent detection for optical OFDM systems before down conversion.

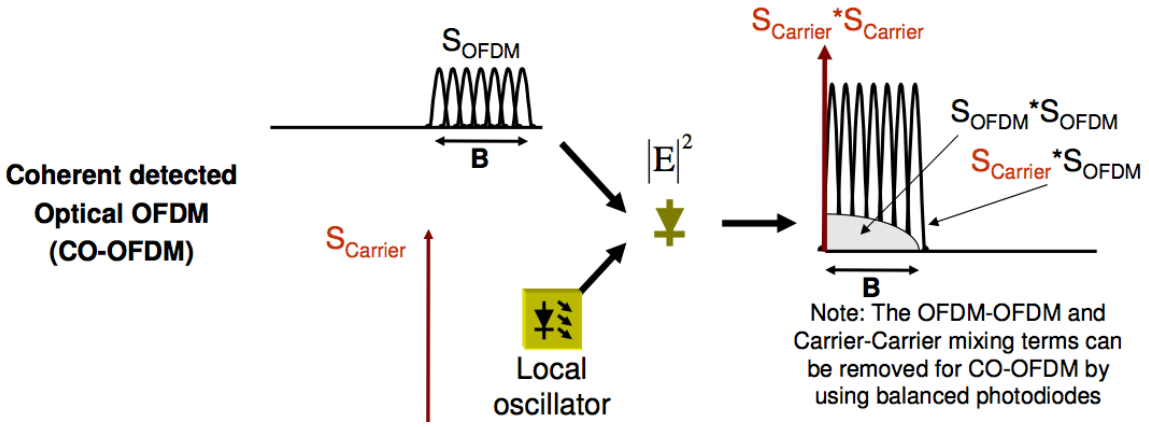

Figure 2 Coherent detected optical OFDM (taken from [56]).

2.2. Phase noise

From the previous section, it is obvious that CO-OFDM systems require a coherent receiver, meaning that the optical carrier has to be generated locally by a laser before photon detection. Thus, these systems are sensitive to the laser phase noise [61].

In coherent optical communication systems, laser phase noise is caused by instabilities in the two required oscillation sources — the laser of the transmitter and the local oscillator

(LO) laser of the receiver [62], [63].

Laser phase noise manifests through the broadening of the spectral linewidth. It is usually modeled as a Wiener process [61][64]. Instead of only single frequency, the output of a laser has multiple frequencies, presenting a linewidth ranging from several hundreds of kHz to several MHz. In a transmission system with laser phase noise, the equalizer has to compensate for the receiver phase noise, channel distortions, and also transmitter phase noise [63], [61].

The impact of phase noise on systems using OFDM appears mainly in two forms: 1) it causes a phase rotation of an OFDM symbol, which is common to all subcarriers, and is called common phase error (CPE); 2) it causes a spreading around the central frequency of each subcarrier, leading to adjacent subcarriers interfering with each other, which is referred to as inter-carrier interference (ICI) [64], [34].

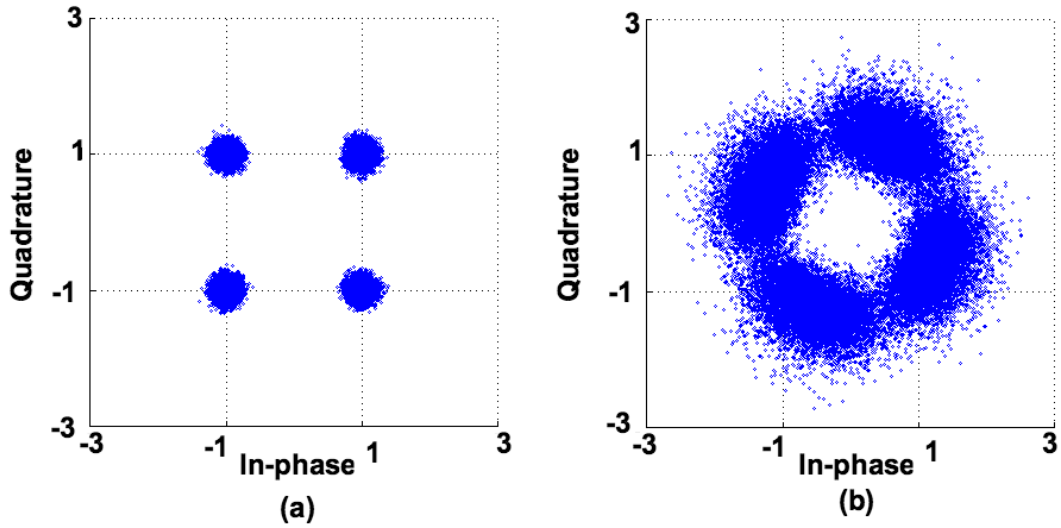

Figure 3 Received 4-QAM constellation: (a) no phase noise (b) with phase noise.

The impact of phase noise on the received constellation of a 4-QAM signal is shown in Figure 3. The phase noise has led to a rotation of the received constellation. In addition, the constellation has become "noisy" due to the ICI. Consequently, it is difficult to process and identify each of the 4-QAM symbols without using effective digital signal processing algorithms for phase noise compensation.

2.3. Channel impairments

The performance of high speed or ultrahigh speed communication systems is constraint by many factors, including phase noise and fiber channel distortions. For communication systems using single mode fiber, the impairments introduced by the optical fiber channel are: fiber attenuation, chromatic dispersion (CD), polarization mode dispersion (PMD), and fiber nonlinearities. Each of the impairments is elaborated in this section.

The propagation of light in the fiber can be modelled by non-linear Schrödinger equation [65]:

$$\frac{\partial A}{\partial z} + \frac{i\beta_2}{2} \cdot \frac{\partial^2 A}{\partial t^2} = i\gamma A|A|^2 - \frac{\alpha}{2} A, \tag{5}$$

where A is the signal amplitude, z is the transmission distance, β_2 is the group velocity dispersion (GVD) parameter, γ is the nonlinear coefficient, and α is the attenuation coefficient, t is time.

2.3.1. Fiber Attenuation

Signal power reduces as it travels through optical fiber because of attenuation. This limits the transmission distance of the signal when using the receiver with the same sensitivity. Fiber attenuation is caused by material absorption and Rayleigh scattering in silica fiber [3]. Material absorption is caused by photo-introduced molecular vibration and impurities introduced during fiber manufacture process. Rayleigh scattering loss is caused by unavoidable microscopic defects and structural inhomogeneities [54]. The specification to describe fiber attenuation profile is attenuation coefficient. Without considering CD and non-linear effects in Equation 5, fiber attenuation can be modelled as:

$$|A(z,t)|^2 = |A(0,t)|^2 \cdot exp(-\alpha \cdot z), \quad (6)$$

where $|A(z,t)|^2$ stands for output power of the signal after a transmission of z, $|A(0,t)|^2$ stands for input power of the signal, α is the attenuation coefficient, and z is the transmission distance. It is obvious that the signal power decreases exponentially as the transmission distance grows.

As the manufacturing technology has been largely improved in recent years, the fiber attenuation has been decreased. This creates three wavelength windows of low fiber attenuation for telecommunications [8], [65]: first window is around 850 nm with an attenuation of 2 dB/km; second window is around 1300 nm with an attenuation of 0.5 dB/km; third window is around 1550 nm with an attenuation of 0.2 dB/km [4], [54]. Figure 4 shows the three telecommunication windows for the new silica fibers, as well as the attenuation characteristic for the silica fiber manufactured before 1980s.

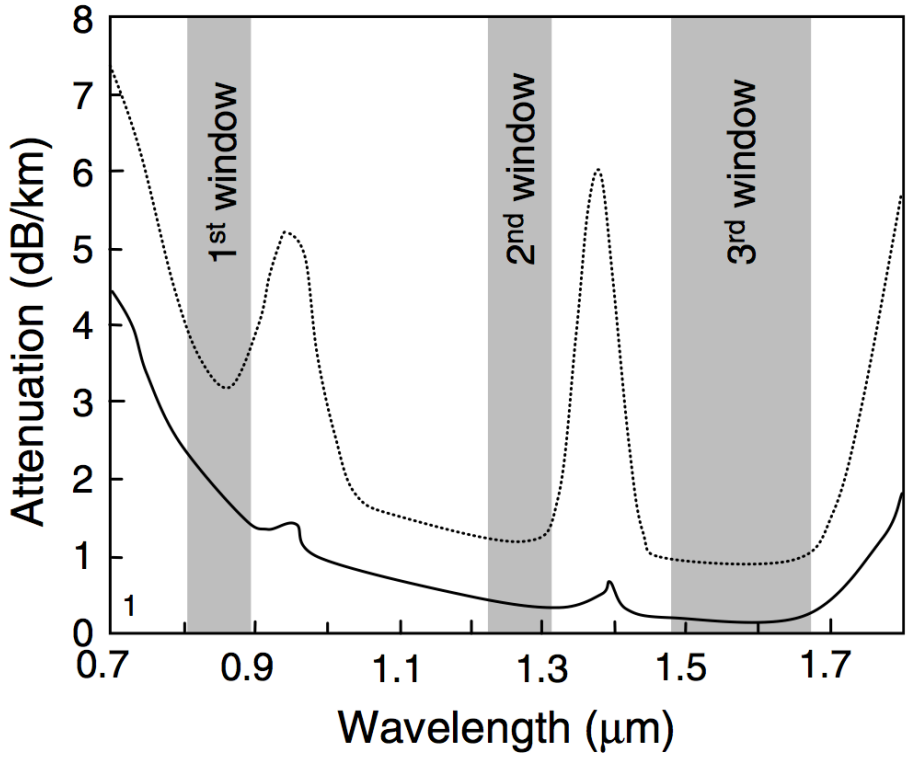

Figure 4 Three telecommunication windows for new silica fiber (solid line) and attenuation for old silica fiber manufactured before 1980s (dotted line) (Fundamentals of Optical Devices, © 2009 Elsevier Retrived from www.knovel.com).

Fiber attenuation is usually compensated by optical amplifiers, such as EDFAs and Ramen amplifiers. However, optical amplifiers introduce additional amplitude noise caused by the amplified spontaneous emission to the system. This decreases the optical signal-to-noise ratio (OSNR). In an optical fiber channel link with optical amplifiers, the OSNR can be defined as [54], [66]:

$$OSNR = \frac{P_S}{2N_A P_{ASE}}, \quad (7)$$

where P_S is the transmitted signal power, N_A is the number of optical amplifiers, and P_{ASE} is the spontaneous emission noise power.

The relationship between OSNR and SNR is defined as [67]:

$$OSNR = \frac{pR_s}{2B_{ref}} SNR, \quad (8)$$

where p indicates the polarization multiplexing of the signal: p equals to 1 if the signal is a singly polarized; p equals to 2 if the signal is a polarization multiplexed. R_s is the symbol rate of the data, B_{ref} is the reference bandwidth for the noise. The typical value of the reference bandwidth is 12.5 GHz, which corresponds to a 0.1 nm resolution bandwidth of an optical spectrum analyzer at 1550 nm carrier wavelength.

2.3.2. Chromatic Dispersion

Chromatic dispersion refers to the phenomenon that different spectrum components of the signal travel at different velocities in optical fiber [54].

Chromatic dispersion happens because of the characteristics of the optical media that when propagating, the phase velocity and the group velocity of light depend on the optical frequency or the wavelength of the light. Group delay is defined as the first derivative of the optical phase with respect to the optical frequency, and chromatic

dispersion is defined as the second derivative of the optical phase with respect to the optical frequency [10], [54].

Without considering fiber attenuation and nonlinearities in Equation 5, the non-linear Schrödinger equation, the frequency domain solution of the equation is [68]:

$$A(z,\omega) = A(0,\omega)\exp\left(\frac{i\beta_2 w^2}{2}z\right), \tag{9}$$

where A is the signal amplitude, z is the transmission distance, ω is the optical angular frequency, β_2 is the GVD parameter, and t is time. GVD describes the time delay accumulated over a certain distance by two spectrum components. It is obvious that different frequency components have different phase shifts. This phase shift causes the signal pulse broadening and interfering with the adjacent symbols, and thus the ISI.

Chromatic dispersion is also evaluated by dispersion parameter D, indicating the time delay after propagating in the fiber for certain length in regard of the wavelength difference between two pulses. The relationship between β_2 and GVD is [6]:

$$D = -\frac{2\pi c}{\lambda^2}\beta_2, \tag{10}$$

where λ is the wavelength of the optical carrier. It can be seen clearly from Equation 10 that dispersion is wavelength dependent. The unit for dispersion parameter D is ps/nm/km.

Chromatic dispersion consists of the waveguide dispersion and the material dispersion [10].

Material dispersion is the result of the electromagnetic absorption, which will lead to the changes in the refractive index of the medium with the changes in optical wavelength [1], [10]. To be more specific, larger wavelength components travel faster than smaller wavelength components. All optical signals have a range of wavelengths, therefore, CD is prevalent.

Waveguide dispersion is due to the speed of a wave in a waveguide depending on its frequency for geometric reasons, independent of any frequency dependence of the materials [3]. It is very often that the electric and magnetic fields of core and cladding are overlapping at the contact area. The amount of the overlapping of the fields is wavelength dependent [1], [3]. That is why the core radius and index difference of a fibre will affect the waveguide dispersion. Considering only waveguide dispersion, shorter wavelength components travel faster than longer wavelength components.

The chromatic dispersion for standard single mode fiber at different wavelengths can be seen in Figure 5.

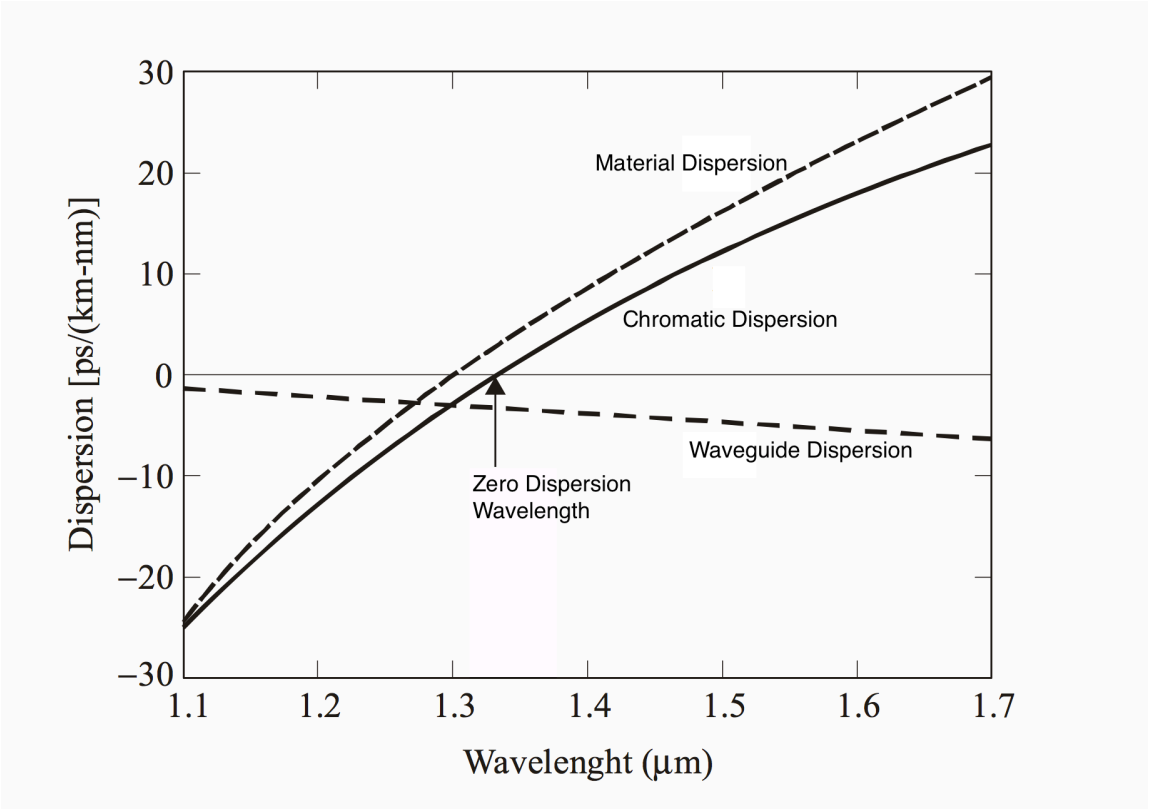

Figure 5 Chromatic Dispersion for standard single mode fiber (reproduced from [11]**).**

It can be seen clearly from Figure 5 that chromatic dispersion is the result of the combination of the effects from material dispersion and waveguide dispersion.

The standard single-mode fibers have zero dispersion at a wavelength of 1310 nm. Also, the chromatic dispersion value is around 16 ps/nm/km at 1550 nm, which is the operation wavelength for practical optical fiber transmission systems. Chromatic dispersion can be compensated by either using dispersion compensation fibers [69], which is usually employed in traditional optical fiber communication systems, or by using a digital filter,

which is used in systems using coherent detection as the detection scheme [69].

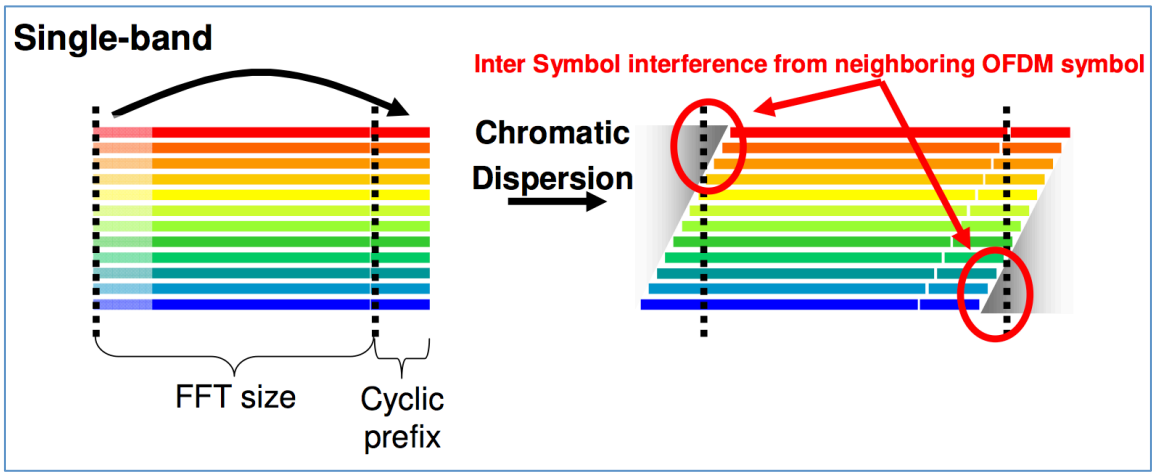

Figure 6 Chromatic dispersion in OFDM systems (reproduced from [56]).

For OFDM communication systems, a simple method to combat CD is to add CP. The CP length should be large enough to cover the ISI. If the CP is not sufficient, ISI appears and compromise the system performance, as has been shown in Figure 6. More sophisticated methods are then required to compensate for CD [70], [71].

2.3.3. Polarization Mode Dispersion

Polarization mode dispersion is dispersion between two orthogonal polarizations of modes. Light waves propagate at different velocities caused by random imperfections and asymmetries in the waveguide of the optical fibers, leading to random broadening of optical pulses [72], [73].

The ideal optical fiber core has a perfectly circular cross-section, where the two orthogonal fundamental modes travel at the same speed. The realistic fibers have random imperfections such as the circular asymmetries or the geometric asymmetry (slightly elliptical cores) and the stress-induced material birefringences [72], causing the two polarizations to propagate at different speeds. The pulse spreading effects in the optical fiber is shown in Figure 7.

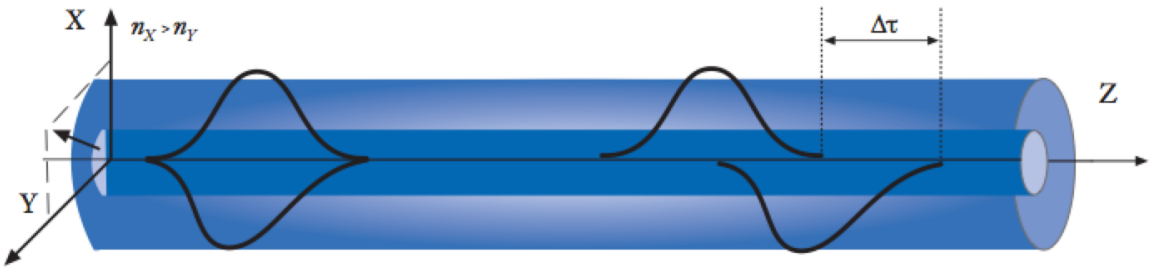

Figure 7 Polarization Mode Dispersion in Optical Fibers (reproduced from [74]**).**

Polarization mode dispersion is measured by the root mean square time average of differential group delay (DGD), the time difference between the two principal states of polarizations [73]. It is proportional to the square root of propagation distance. The unit of the polarization mode dispersion is $ps/\sqrt{km}$.

The common way to compensate polarization mode dispersion is to use a polarization controller to mitigate the differential group delay occurring in optical fibers [75]. Since the polarization mode dispersion effects are random and time-dependent, an active feedback device over time is generally required, in which case systems are more

complicated.

In the early years of the optical fiber manufacturing, PMD could be compensated by using the adaptive filters in digital signal processing for coherent optical communication systems [76], [77].

2.3.4. Non-linear effects

Since light waves are propagating over long distance of optical fibers, the small effects are building up and affect the system performance significantly at certain point. The transmission nonlinear impairments regarding to long-haul high data-rate optical fiber communication systems usually include the fiber Kerr nonlinearities, the self-phase modulation (SPM), the cross-phase modulation (XPM) and the four-wave mixing (FWM) [46], [78].

Generally speaking, the signals propagating through the optical fibers suffered from attenuation, chromatic dispersion and nonlinear effects follow the nonlinear Schrödinger equation. By ignoring the chromatic dispersion in Equ 5, the non-linear Schrödinger equation, the equation can be simplified as [79]:

$$A(z,t) = A(0,\omega)\exp\big(i\Phi_{NL}(z,t)\big), \tag{11}$$

where $\Phi_{NL}(z,t)$ is the non-linear phase, which can be expressed as:

$$\Phi_{NL}(z,t) = \gamma \int_0^z |A(z',t)|^2 dz', \tag{12}$$

where γ is the non-linear coefficient. The nonlinear parameter depends inversely on the effective core area of the transmission fiber, defined as [11], [46]:

$$\gamma = \frac{\omega \eta_2}{c A_{eff}}, \tag{13}$$

where γ is the non-linear coefficient, ω is the optical frequency, η_2 is the non-linear refractive index, c is the speed of light, and A_{eff} is the effective area of the optical fiber core.

The solution of Equ 12 is [11], [46]:

$$\Phi_{NL}(z,t) = \gamma |A(0,t)|^2 \frac{(1 - \exp(-\alpha z))N_A}{\alpha}, \tag{14}$$

where N_A is the number of optical amplifiers. It is obvious that the phase shift of the signal is proportional to the power of the signal. This relationship is non-linear. Hence the nonlinearities of the fiber.

The systems which employs wavelength division multiplexing, suffer from inter-channel interference and intra-channel interference in regard to non-linearities. Inter-channel nonlinear effects is the interference between different wavelength channels, which include the cross-phase modulation (XPM) and the four-wave mixing (FWM); Intra-channel nonlinear effects indicate the interference between different modules in the same

wavelength channel, which include self-phase modulation (SPM), intra-channel XPM and intra-channel FWM. Inter-channel nonlinearities are important for lower bit-rate transmission systems, while intra-channel nonlinearities are more important for high bit-rate transmission systems.

When using traditional high data rate optical transmission systems, which employ intensity modulation direct detection, the compensation for nonlinear effects are relatively complicated; while in digital systems using coherent detection scheme, the nonlinear effects can be compensated by using the backpropagation based on solving the nonlinear Schrödinger equation.

2.4. Chapter Summary

In this chapter, different detection schemes for optical communication systems are introduced, as well as the comparison between single carrier and OFDM. The conclusion is that CO-OFDM is an appropriate choice for long-haul communication and phase noise is a prominent problem in these systems. The cause and effects of phase noise is discussed. Also, single mode fiber channel impairments including CD, PMD, and nonlinearities are explored. All these contribute to the overall CO-OFDM system impairment and limit the system performance.

Chapter 3 Channel Impairments Compensation for Long-haul CO-OFDM systems

In this chapter, the compensation methods for the major impairments in optical fiber are explored. A long-haul CO-OFDM system is designed and simulated to explore the effects on system performance from the optical fiber, as well as the effectiveness of the chosen compensation methods for different impairments. Simulation results are presented and discussed for compensation of fiber impairments.

Fiber attenuation is compensated by an EDFA after every 80 km of SSMF. For CD compensation, simply using CP (cyclic prefix) is compared with overlap-and-save CD compensation method. Then the effects of PMD on the system are simulated and a simple way to compensate is provided: 1-tap equalization. The performance degradation from non-linear effects is then discussed and simulation result shows that by changing the fiber launch power, the impact on system BER from nonlinearities can be reduced.

3.1. Long-haul CO-OFDM system simulation setup

In order to explore the channel impairments of the long-haul CO-OFDM communication systems, a typical system is set up and simulated in MATLAB and VPItransmissionMaker^{TM}OpticalSystems (VPI is the abbreviation used in this thesis).

VPI helps to design new optical communication systems with different ranges, including long haul. It also supports upgrading existing network through component substitution [80]. It has built-in modules as well as custom modules, which allow co-simulation with MATLAB, Python, and C++ [81]. In this thesis, MATLAB and VPI built-in and custom modules are used for simulations.

This research work, as a part of the OmOptics Project, focuses on the phase noise compensation methods: RF-pilot compensation method and common phase error compensation method, while considering the mitigation of optical channel impairments. Figure 8 shows the system block diagram for the long-haul CO-OFDM communication system designed for this work. As can be seen from Figure 8, if using RF-pilot method for phase noise compensation, the compensation action should be before serial-to-parallel conversion and FFT; if pilot-aided CPE method is used for phase noise compensation, the compensation action should be after FFT and channel equalization.

The system consists of a transmitter, an optical channel, and a receiver. The digital signal processing part for both the transmitter and receiver are simulated in MATLAB. The optical channel and the rest of the transmitter and receiver are simulated in VPI.

Digital transmitter generates digital OFDM signals. These signals then go through digital-to-analog converter (DAC) and MZMs. The resulting optical signals are fed to the optical fiber. After the fiber, the distorted signals are received by a coherent optical receiver. The resulting electrical signals are then converted back as digital signals and processed by the

digital OFDM receiver with algorithms to compensate CD effects, PMD effects, and phase noise compensation. Bit error rate (BER) is the measurement of system performance. The details for simulation setup are presented in the next two subsections.

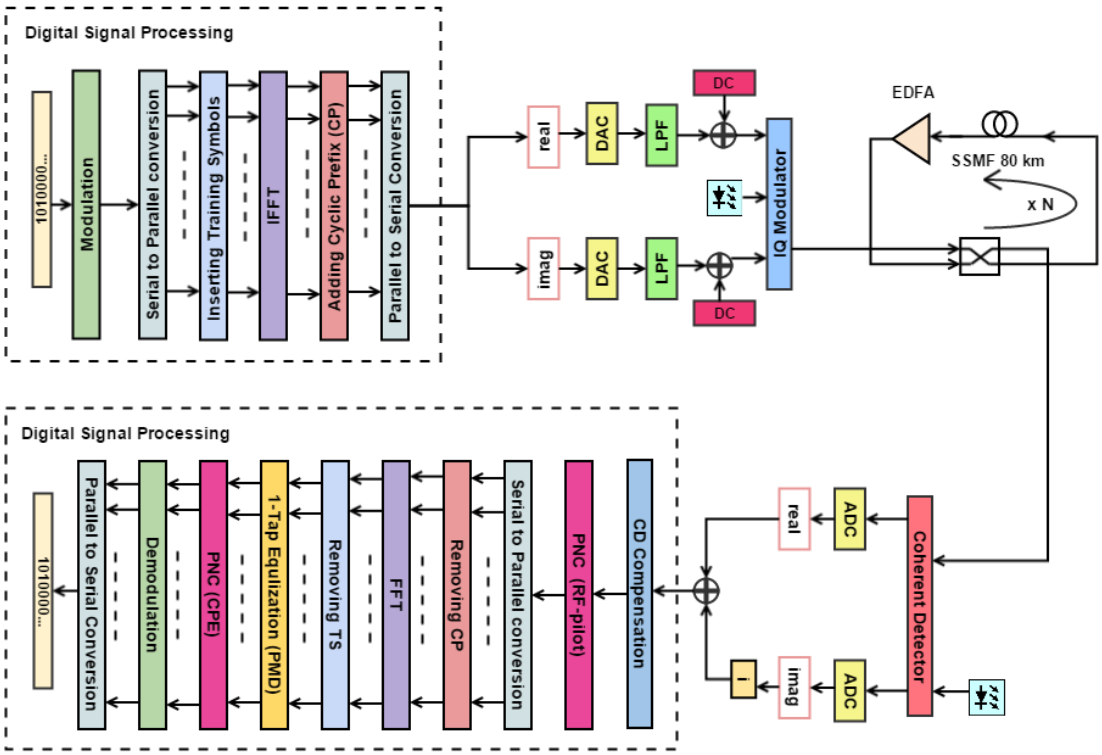

Figure 8 System block diagram for CO-OFDM system.

3.1.1. Simulating digital Tx and Rx using Matlab

The digital transmitter generates digital OFDM signals and saves the signals as real part and imaginary part separately, ready to be used for further processing in VPI.

The digital transmitter generates a random sequence of bits, with equal probabilities for

ones and zeros, as the information source. Then the data sequence is modulated as 4-QAM. These symbols pass a serial to parallel converter. With inserted training symbols for channel equalization, an IFFT is applied to generate the OFDM symbols. The OFDM signal is generated using an IFFT/FFT with a 5.47% cyclic prefix (CP). The reason to use a small CP is that a sophisticated chromatic dispersion compensation method, overlap-and-save method, is employed in the system. This method requires a small percentage of CP. Details of this method are discussed later in this chapter. IFFT/FFT size is 128. Common FFT size ranges from 128 to 1024. Smaller FFT size has the advantage of less processing complexity and less sensitivity to laser phase noise when using coherent detection. A hundred subcarriers are used for data in this chapter to increase bandwidth efficiency.

The sampling rate of the digital-to-analog converter (DAC) is 40 GS/s, resulting in a a data rate of 64 Gbit/s, using 4-QAM as the modulation format and 100 data subcarriers out of total 128 subcarriers. Higher data rate can be easily reached when employing WDM.

After this, cyclic prefix is added to combat inter-symbol interference (ISI) caused by chromatic dispersion (CD) from the optical fiber channel. Finally, these OFDM symbols pass through the parallel to serial converter for further processing in VPI.

The digital receiver receives the data from VPI, compensates for the fiber impairments as well as the phase noise, and recovers the data sequence from the OFDM symbols.

However, the recovered data will still contain error. Comparing the recovered information bits and the transmitted ones, the ratio between the number of error bits to the total number of transmitted bits is the system BER and it is used as a metric for system performance.

At the digital receiver side, a frequency-domain equalizer using the overlap-add method [82] is utilized at the receiver side for CD compensation. The principles and performance of this compensation method is elaborated in the next section. For phase noise compensation, there are RF-pilot method and pilot-aided common phase error (pilot-aided CPE) method. Both methods are explained and compared in detail in Chapter 4. If using RF-pilot method, the compensation is performed right after CD compensation. Then serial-to-parallel conversion is performed, preparing the data for CP removal and FFT. After FFT, training symbols (TSs) are removed to get channel response and compensate for it by 1-tap equalization. PMD is also mitigated during this process. If pilot-aided CPE method is used for phase noise compensation, the compensation action follows 1-tap equalization. Then, the data is demodulated and converted to serial. This recovered information sequence is then compared with the original transmitted one, calculating the system BER, as has been explained previously.

3.1.2. Simulating optical channel and components using VPI

The rest of the system is simulated in VPI. Figure 9 shows the VPI schematic for the CO-OFDM system excluding the digital signal processing operations. The in-phase and

quadrature part of the OFDM signal are extracted from VPI schematic input folder, which holds the data from the digital transmitter. These data are modulated by Mach-Zehnder modulator (MZM) separately, and then combined again, as illustrated in the block diagram in Figure 8, and then sent to the optical fiber channel.

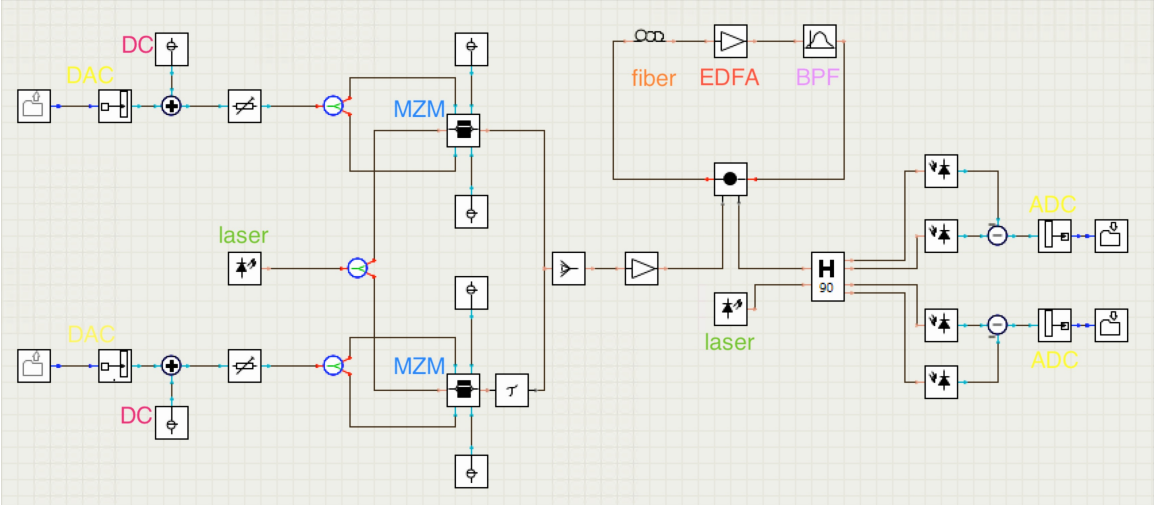

Figure 9 VPI schematic for optical channel and components.

The long-haul optical channel consists of multiple loops. Each loop consists of an 80 km span of standard single mode fiber (SSMF), followed by an erbium doped fiber amplifier (EDFA) and a band-pass filter (BPF). EDFA is used to compensate for fiber attenuation and BPF here is used to filter out out-of-band noise. The SSMF parameters are: an attenuation of 0.2 dB/km, chromatic dispersion (CD) parameter of 16 ps/nm/km, and non-linear coefficient of $2.6\times10^{-20}\ s^2/W$. Attenuation is compensated by an amplifier with 16 dB gain and a noise figure of 4 dB within each fiber loop.

A coherent receiver with balanced photodiodes follows the output of the fiber. Balanced photodiodes are used to cancel the local oscillator to local oscillator mixing and signal to signal mixing, as has been discussed in previous section about coherent detection. Also, by suppressing components like DC, balanced photodiodes setup improves local oscillator to signal power ratio, helping system performance [9],[56]. Then the data are saved for further DSP of the digital receiver mentioned in Section 3.1.1.

In this chapter, lasers with 100 kHz linewidth are employed at both transmitter and receiver. This is a reasonable choice considered the price of the laser and the communication system that was of interest here. Conventional DFB lasers have larger laser linewidths as large as several MHz. Narrow linewidth lasers like ECL lasers, having linewidths ranging from 10kHz to 800 kHz, are generally more expensive and have more systems restrictions regarding FFT when using OFDM. Also, OmOptics Project has purchased a laser with 100 kHz laser linewidth. The results presented in the thesis can be verified through experimentation. RF-pilot phase noise compensation method is used to mitigate the phase noise distortions. This method is elaborated in Chapter 4.

3.2. CD compensation

Frequently, CD compensation methods can be categorized into time-domain CD equalization and frequency-domain CD equalization. Theoretically, ISI caused by CD can be compensated with an extended CP. However, larger CP consumes more useful bandwidth. A preferred way to compensate for CD is to use overlap-and-save CD

compensation method. In this section, the system performance from both methods are shown and compared.

3.2.1. CP based CD compensation

Figure 10 shows the system BER change against OSNR change. The fiber length is 20 km in this case and no optical amplifier is used. The case of using no CP is shown in the figure as a reference to show the CD impairments.

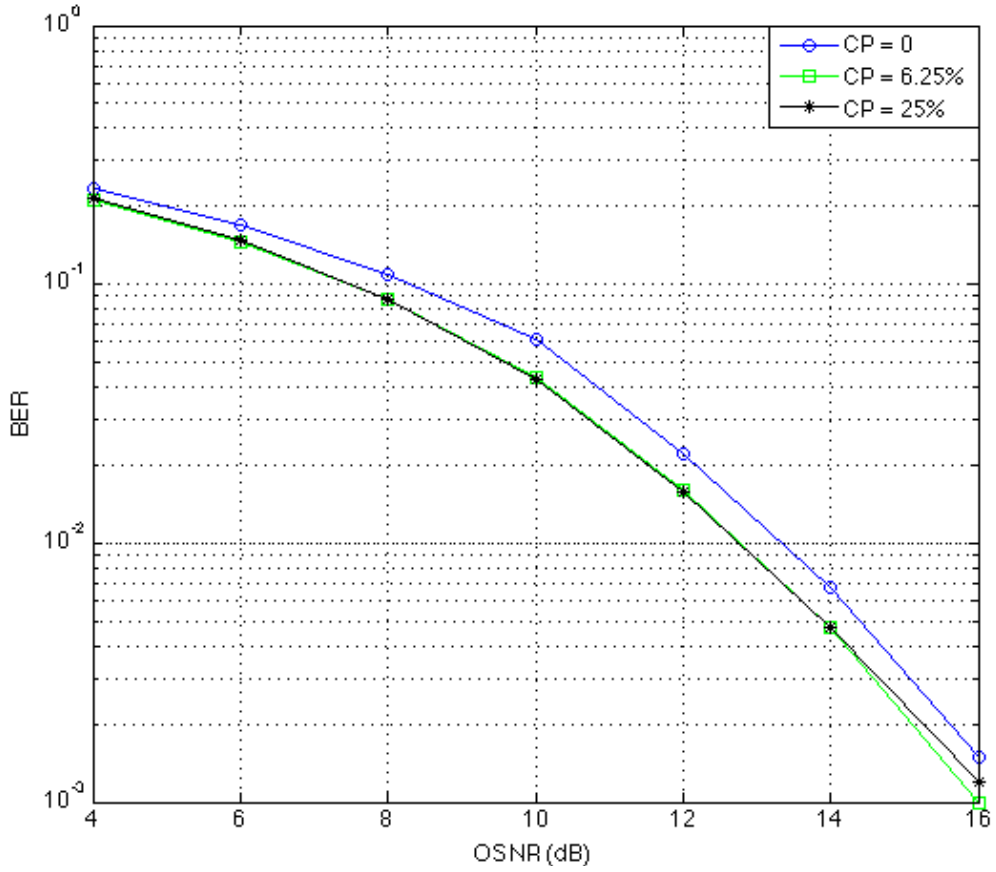

Figure 10 BER vs. OSNR with 20 km SSMF.

As can be clearly seen, the system BER decreases when OSNR is increased, which is expected. Only a 6.25% CP can improve the OSNR by ~0.7 dB at a BER of 2×10^{-2}. Further increasing the CP length to as large as 25% almost has almost no impact on system BER. Here, 2×10^{-2} is the so-called "forward error correction (FEC) threshold".

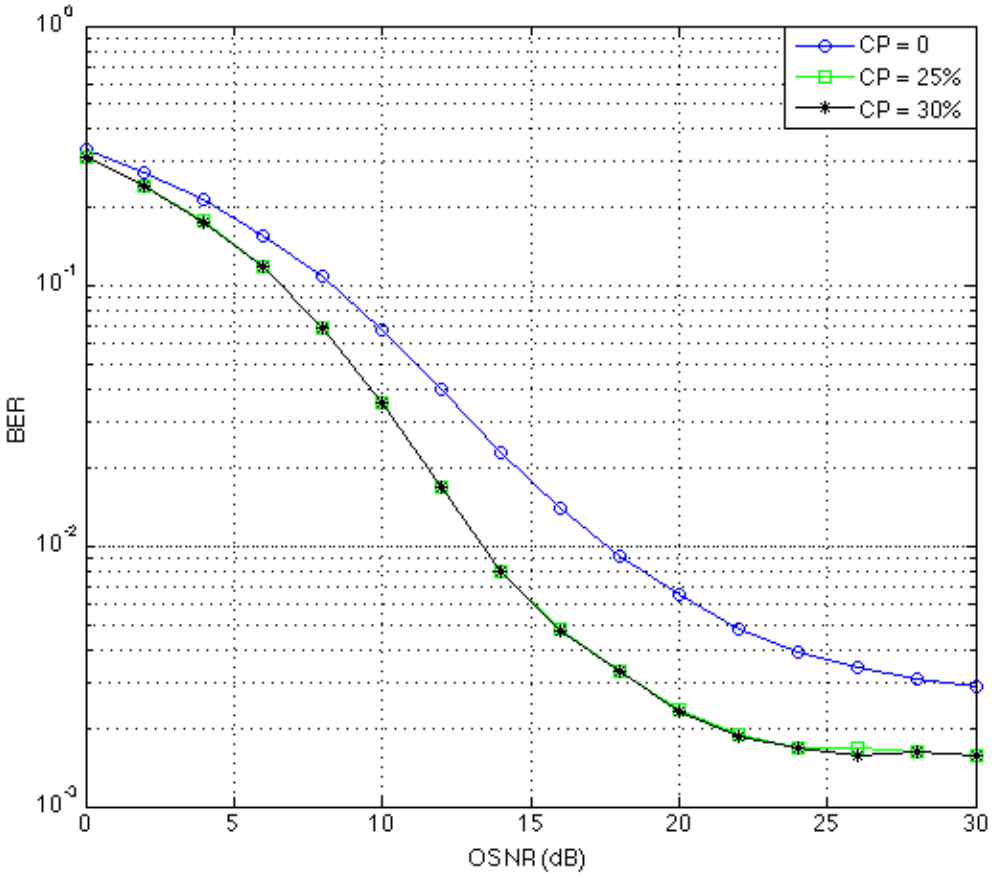

Figure 11 BER vs. OSNR CP with 80 km SSMF.

FEC threshold is the simulated system BER without FEC coding and decoding. Assuming the system BER with the help of FEC is only dependent on the system BER

without coding, the post-FEC should help reduce the system BER to a desired level, as low as 10^{-12} or 10^{-15} in optical communications with certain code rate and overhead. When the fiber length is increased to 80 km, as is shown in Figure 11, it can be seen that insertion of 30% CP has almost no improvement on system BER. Further increasing the CP length introduces an even lager overhead without significant improvement on system BER. Larger fiber lengths would further exacerbate this problem, thus making use of CP ineffective. A more sophisticated method has to be introduced. The preferred method in this work is overlap-and-save CD compensation. The performance of this method is introduced in the next subsection.

3.2.2. Overlap-and-save CD compensation

In Chapter 2, we stated that CD is deterministic, and so fixed equalizers can be used to compensate for CD effects. Fixed equalizers can be implemented with filters having fixed coefficients. It is possible to use a time-domain equalizer (TDE) with a finite impulse response (FIR) fixed filter [83] or a frequency-domain equalizer (FDE) with fixed coefficients filter to combat impairments caused by CD [84], [85].

From Equation 8 in Chapter 2, it is obvious that CD affects all frequency components. The transfer function of CD effects essentially corresponds to an all-pass filter. As long as the transmission distance of the optical fiber is known, the amount of CD impairment can be calculated, and its effects can be reversed by applying a fixed equalizer.

For long-haul optical transmission, the complexity of the compensation procedure increases with the transmission distance for TDEs [78]. FDEs are often used. Here, overlap and save method is explained and used in the simulation.

Overlap-and-save CD compensation method [78], [86] is a frequency-domain CD compensation method. Figure 12 shows the overlap-and-save CD compensation procedure for OFDM systems [87], [88].

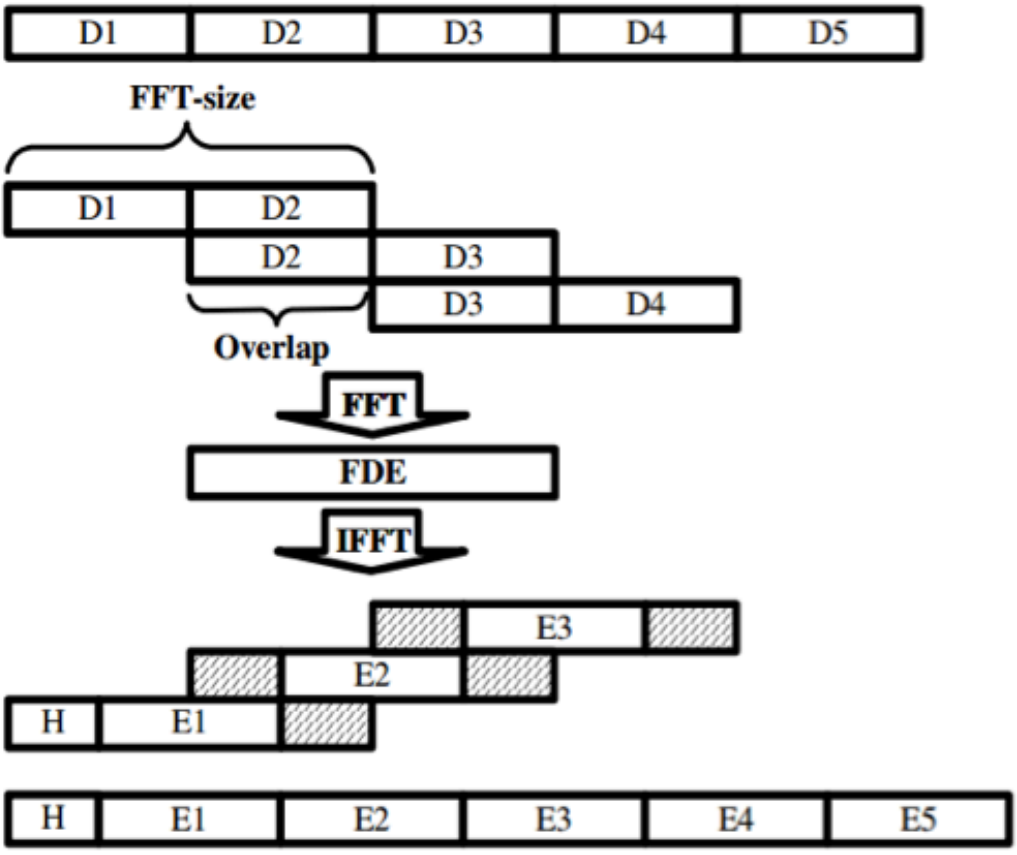

Figure 12 Overlap-and-save CD compensation for OFDM systems (reproduced from [70]).

At the receiver side, the data is divided into groups half the size of FFT: D_1, D_2, D_3, D_4, and D5. Then they are combined into groups that have overlapping parts: D_1+ D_2, D_2+D_3, D_3+D_4, and so on. The overlapped groups are then applied with FFT operation. The frequency domain data are multiplied by the conjugation of Equation 8, and then transferred back to time domain data by IFFT operation. The time domain data are combined together after eliminating the bilateral overlapped parts: E_1, E_2, E_3, E_4, E_5.

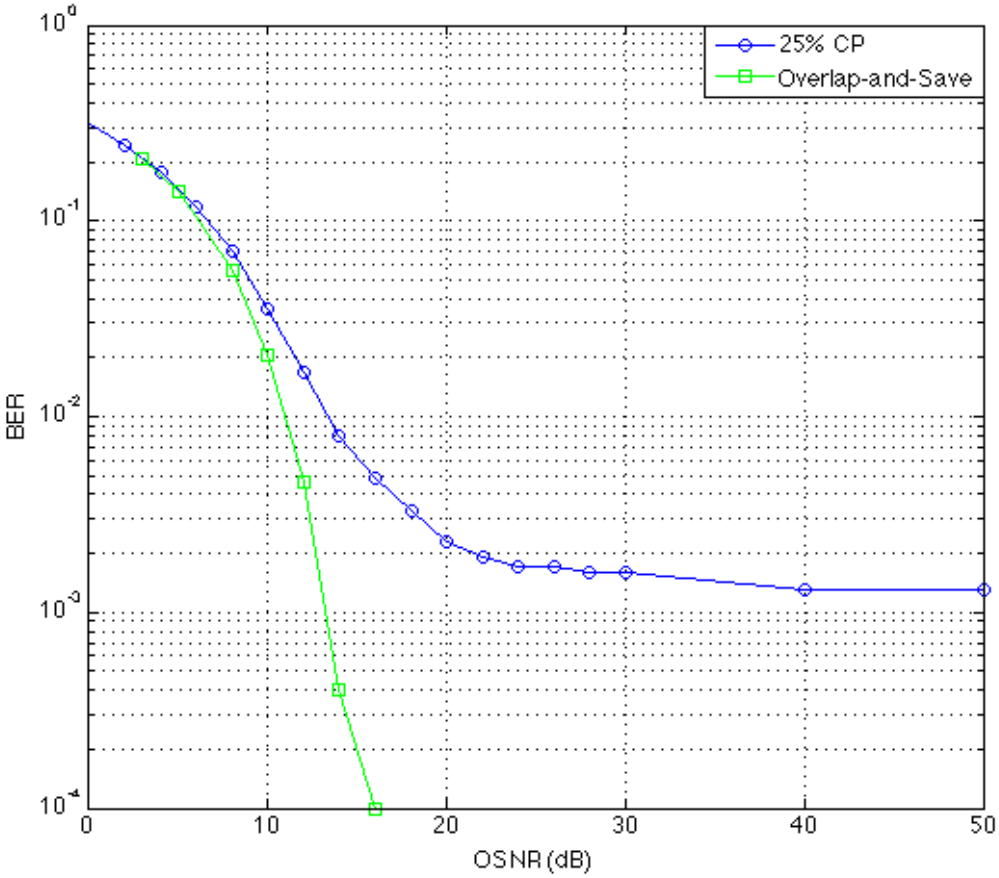

Figure 13 BER vs. OSNR with different CD compensation methods.

Figure 13 shows the system BER performance comparison for using only CP and overlap-and-save method for combating CD effects.

The fiber length in this figure is 80 km, and no optical amplifier is used. PMD is not considered in this case. As can be seen clearly from Figure 13, though a large CP is employed (25% CP), the system BER shows an error floor when OSNR increases. The system BER remains larger than 10^{-3}. As a comparison, when using overlap-and-save CD compensation method, the system BER shows a sharp drop with increased OSNR. It reaches a BER of 10^{-3} easily at an OSNR of ~13 dB and reaches a BER of 10^{-4} at an OSNR of ~16 dB.

Overlap and save CD compensation method clearly has a superior system BER performance at the cost of increased system complexity.

3.3. PMD compensation

PMD should also be considered in a long-haul CO-OFDM system, as has been explained in Chapter 2. In this section, same simulation parameters are used as in Section 3.2.2. Overlap-and-save CD compensation method is used. Figure 14 shows the system BER against the OSNR with and without the impact of PMD. Both curves show the same trend. However, at any given BER, the OSNR penalty of the system with PMD is larger than 4 dB. It is important to compensate for PMD at the receiver side. One simple method is to use 1-Tap equalization.

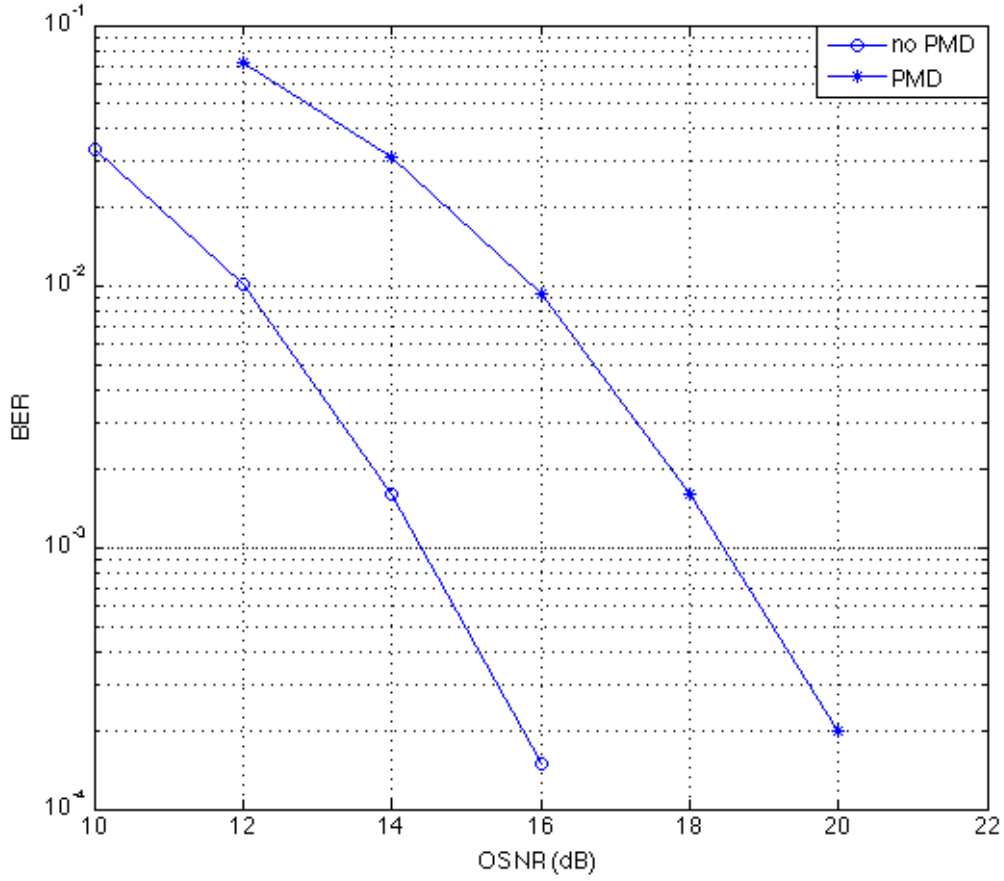

Figure 14 BER vs. OSNR with and without PMD.

At the transmitter side, before the IFFT action, training symbols that have the same OFDM symbol duration are inserted in the data block. These training symbols are evenly spaced throughout the data block. They go through the optical fiber channel with the OFDM symbols. At the receiver side, the distorted training symbols are examined after FFT in the frequency domain, as has been shown in Figure 8. Channel response is obtained by division of the received training symbols and transmitted ones. Then the

conjugation of the estimated channel response is applied to the data as compensation.

Inserting more training symbols gives a more accurate estimate of the channel condition. However, this also results in a larger system redundancy. It is important to explore the necessary training block redundancy.

Training block redundancy is defined as:

$$\boldsymbol{\varepsilon_{TS}} = \frac{\mathbf{1}}{\boldsymbol{N_{TS}}}, \tag{15}$$

in which ε_{TS} means training symbol overhead, and N_{TS} means average training symbol space. A training block usually consists of two OFDM training symbols.

In this section, each training block has the length of one OFDM symbol. Figure 15 shows the compensated performances with various training symbol insertion frequencies: every 200 OFDM symbols, every 100 OFDM symbols, and every 50 OFDM symbols. In all cases, the system BER drops as OSNR increases, as expected. To reach a certain BER, 2×10^{-2} for instance, using every 200 OFDM symbols insertion frequency as a reference, using every 100 OFDM symbols insertion frequency shows ~1.5 dB OSNR improvement and using every 50 OFDM symbols insertion frequency shows ~3 dB OSNR improvement. Apparently, every 50 OFDM symbol case is preferable. The training block overhead corresponding to one TS every 50 OFDM symbols is 2% and is used in later simulation results.

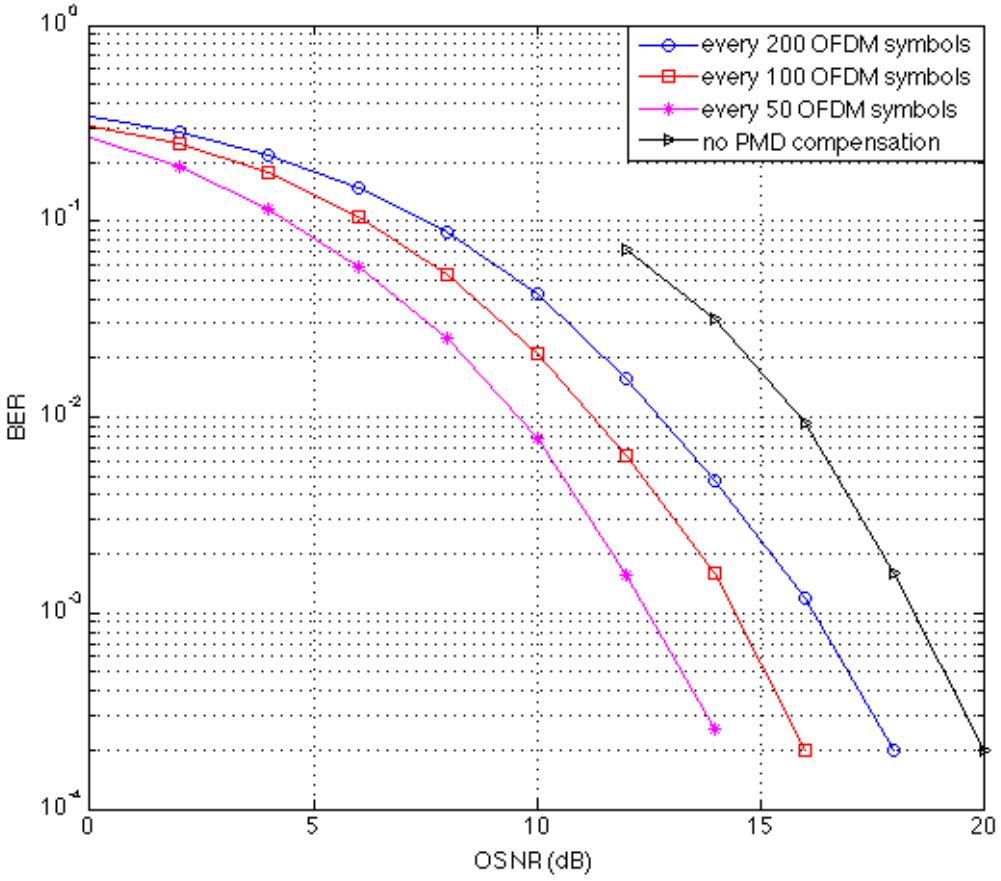

Figure 15 BER vs. OSNR with various number of TSs.

3.4. Non-linear effects

Fiber launch power is a critical parameter for a long-haul transmission system. A low fiber launch power leads to a low received power, yielding poor system performance. On the other hand, a high fiber launch power may cause severe fiber nonlinear effects, distorting the signals.

Figure 16 shows the BER as a function of the launch power after 430-km standard single-mode fiber (SSMF) transmission.

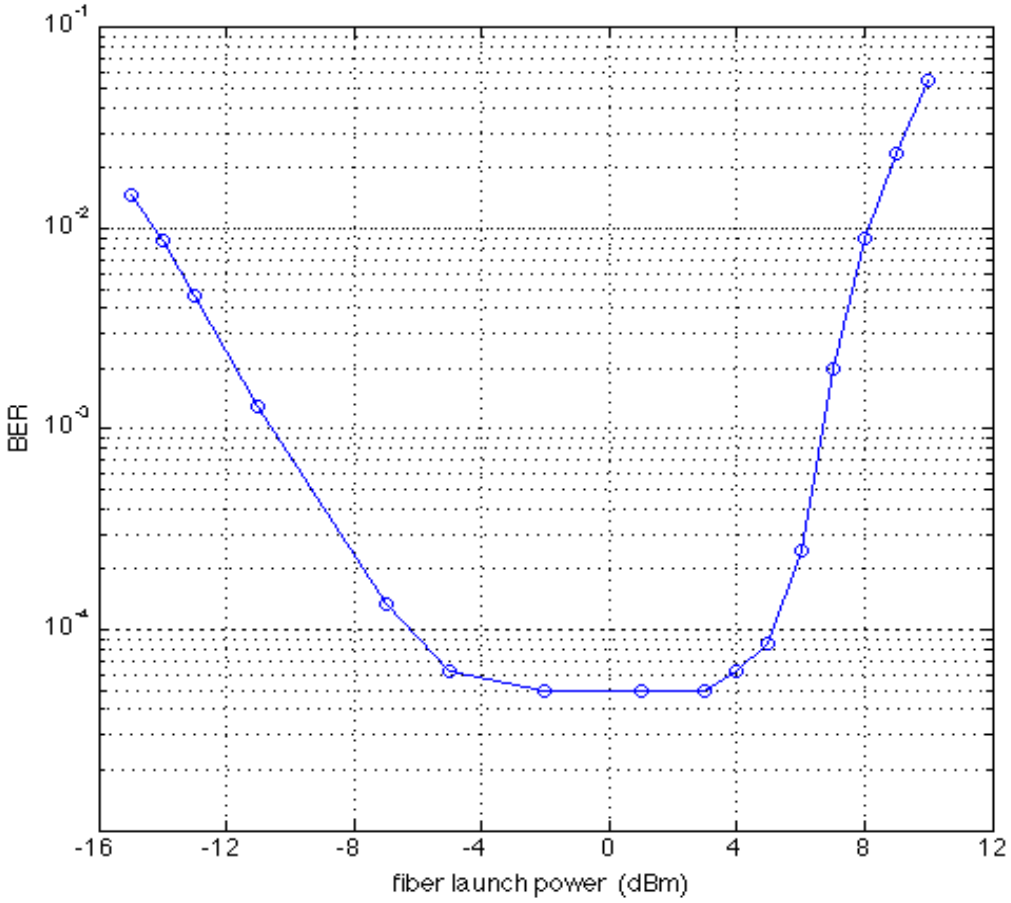

Figure 16 BER vs. fiber launch power.

A frequency-domain equalizer using the overlap-add method [82] is utilized at the receiver side for CD compensation. Figure 16 shows that the BER performance improves when the fiber launch power is increased beyond -15 dBm, and reaches minimum at 1

dBm. Afterwards, fiber nonlinear effects start to dominate and BER increases.

In this thesis, the fiber launch power in all later simulation results is kept below -10 dBm to avoid severe non-linear effects.

3.5. Chapter summary

In this chapter, a typical coherent optical OFDM system is setup using both MATLAB and VPI to examine the fiber distortions on the system. The digital transmitter is simulated in MATLAB to generate OFDM symbols with cyclic prefix and training symbols. The digital receiver is also simulated in MATLAB to compensate for fiber distortions and recover received OFDM symbols into the binary data sequence. The rest of the blocks in transmitter and receiver, and also the optical fiber channel, are simulated using VPI.

Then this chapter continues to explore the fiber distortions and corresponding compensation methods in detail. Starting with CD effects, its impact, and two different compensation methods are presented and their effectiveness is compared; then PMD's impact on system is shown, as well as the system performance after 1-tap equalization as a compensating method. The chosen parameters for the compensation are explained and justified. The section considers fiber nonlinearities as well. The fiber non-linear effects are limited by carefully choosing fiber launch power, so that the received signal power is high enough, yet not too high to cause server non-linear distortion.

Chapter 4 Phase Noise Compensation in Long-haul CO-OFDM systems

In this chapter, a CO-OFDM system is designed and simulated to explore the effectiveness of different phase noise compensation methods.

The principles of RF-pilot phase noise compensation method and pilot-aided common phase error phase noise compensation method are introduced. Then a CO-OFDM system to explore these methods is designed and the simulation setup is described. Simulation results of the performances of both methods are explored in detail. Finally, comparisons between those methods are provided.

4.1. Phase noise compensation methods

It has been shown with the aid of simulations and experiments that one way to compensate for phase noise in optical OFDM systems is to use pilot-aided CPE method [59], [56]. This method assumes that within an OFDM symbol duration, the phase remains the same for the signal and LO lasers. While this method effectively compensates for the common phase rotation caused by the laser phase noise, it does not mitigate the ICI. In comparison, the RF-pilot phase noise method compensates for both degradations

[89], [90]. Part of this work was presented as a research article at the twenty-third annual Newfoundland Electrical and Computer Engineering Conference in St. John's, Newfoundland, under the category of communication and network in 2014. These results were also presented as a research poster in the fourteenth Canadian Workshop on Information Technology, held in St. John's, Newfoundland, and an article on Optical Express [91] in 2015.

4.1.1. RF-pilot phase noise compensation method

An effective method to compensate for the phase noise is to use RF-pilot [89]. This involves inserting an RF- pilot tone in the center of an OFDM signal. The RF-pilot will have the same degradation as the OFDM signal, and can be used at the receiver side to compensate for the phase noise distortions of the OFDM signal.

Figure 17 shows the optical spectrum of the OFDM signal with the RF-pilot tone inserted.

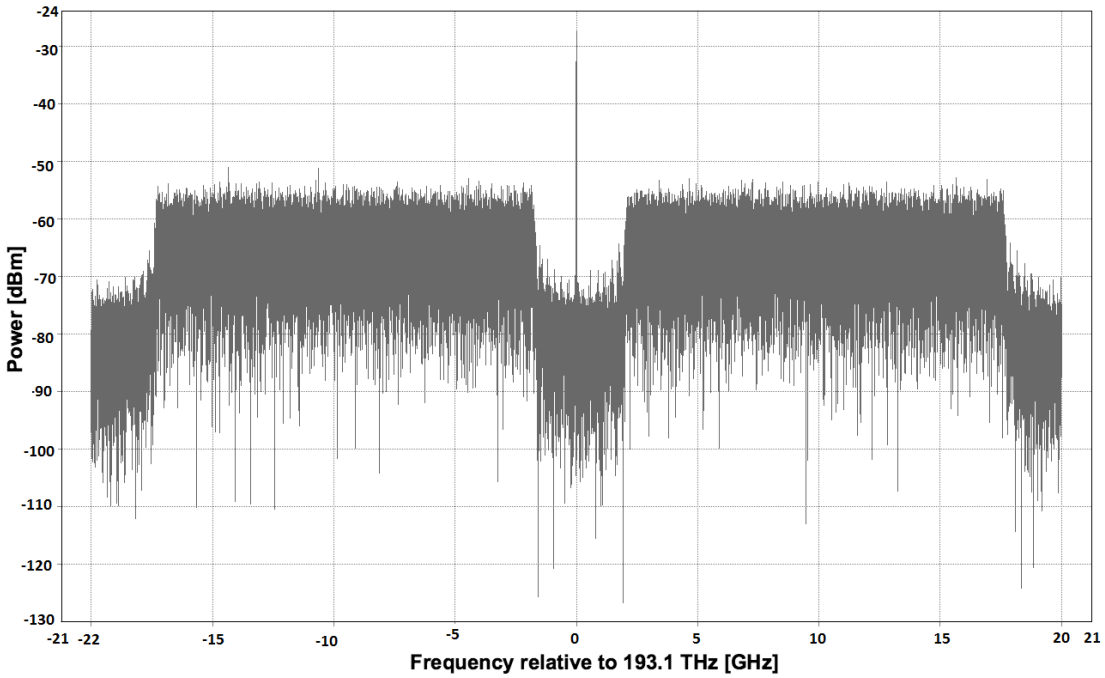

Figure 17 Optical spectrum of CO-OFDM signal with RF-pilot tone inserted.

A DC level is added to the signal in time domain, which corresponds to a sharp pulse

(RF-pilot) in the middle of the OFDM signal in frequency domain. After optical modulator, this sharp impulse is at laser center frequency. The RF- pilot will be distorted by phase noise in exactly the same way as the OFDM signal. At the receiver side, after photo detection, the DSP implementation for compensating for the phase noise involves extracting the RF-pilot from the OFDM signal with a low-pass filter (LPF), applying complex conjugation, and multiplying with the noisy OFDM signal, shown in Figure 18.

In addition, inserted RF-pilot introduces extra power in the system during the entire transmission period, helps to alleviate the PAPR problem resulting from employing OFDM.

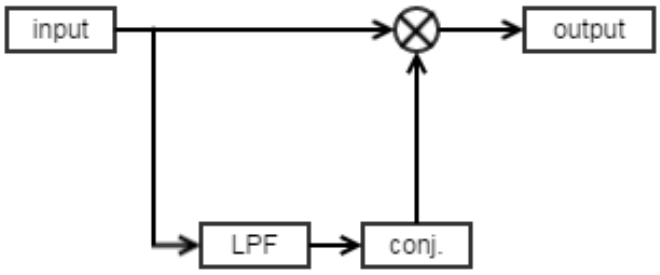

Figure 18 RF-pilot phase noise compensation.

Here, a 128-point IFFT/FFT size is used as an example to show the subcarrier mapping if using RF-pilot method for phase noise compensation. Out of the 128 subcarriers, 100 are used to transmit data, 22 are padded with zeros for oversampling to combat aliasing, and the remaining 6 are used as a guard band between the RF-pilot and OFDM symbol.

The guard band around the RF-pilot is necessary because of the existence of ICI as well as the imperfection of a digital filter that is used to filter out the distorted RF-pilot.

Figure 19 shows how the subcarriers are mapped to the IFFT inputs. 50 data subcarriers are mapped to IFFT inputs 3 to 52, while the remaining 50 data subcarriers are mapped to IFFT inputs 75 to 124. The IFFT inputs from 0 to 2, as well as the inputs from 125 to 127 are assigned to the zero-valued tones that act as the guard band. This implies that the IFFT inputs from 53 to 74 are assigned to the zero-valued tones that are used for oversampling.

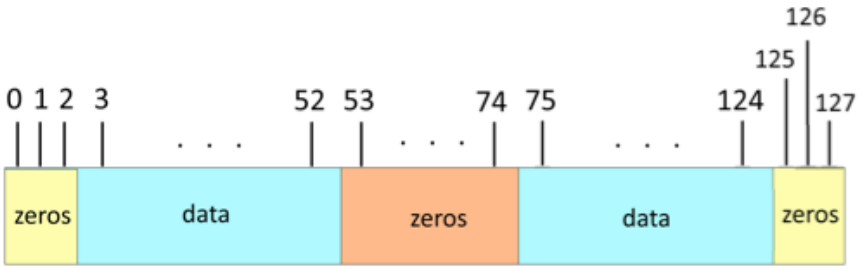

Figure 19 IFFT/FFT subcarrier mapping.

4.1.2. Pilot-aided common phase error phase noise compensation method

On the other hand, when using pilot-aided CPE method for phase noise compensation, the mapping is slightly different. The subcarriers reserved for the guard band for RF-pilot are used for pilots. Figure 20 shows the IFFT mapping comparison. In this figure, from center to right, the IFFT number ranges from 0 to 63; from left to center, the IFFT number

ranges from 64 to 127. Both methods have five subcarriers for phase noise compensation as an example. Different from the RF-pilot method, the five subcarriers for the pilot-aided CPE compensation method are actually occupied by known data as pilots. At the receiver side, after FFT and channel equalization, those pilots are used to correct the common phase rotation, as has been discussed in Chapter 2.

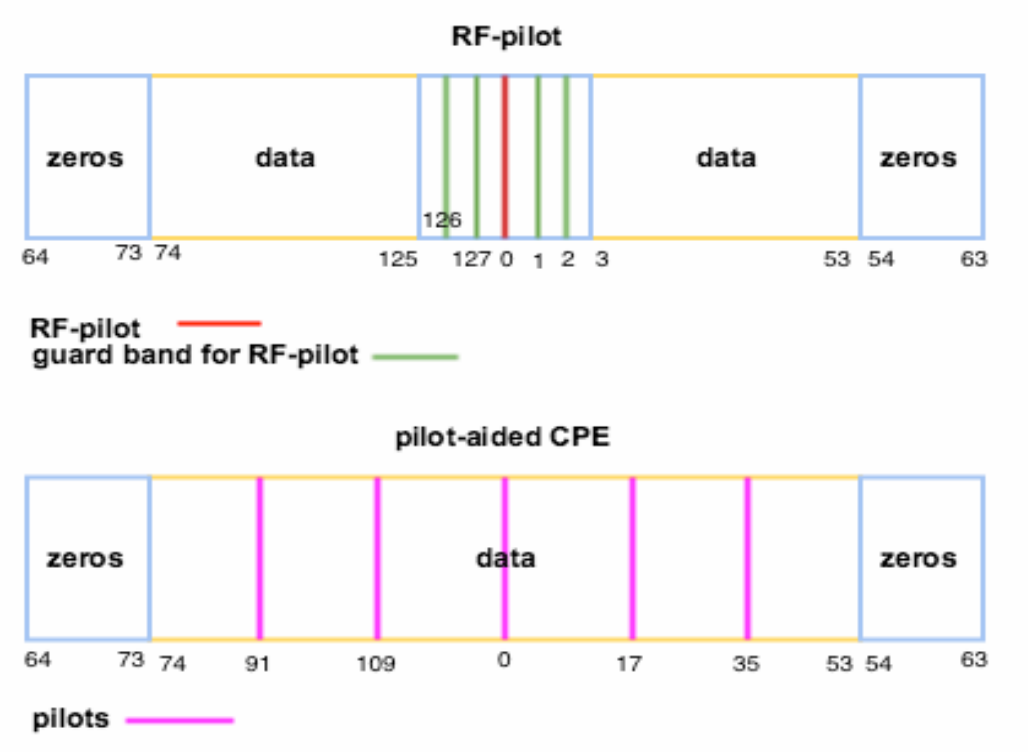

Figure 20 IFFT mapping for pilot-aided CPE method and RF-pilot method.

For pilot-aided CPE method, the system distortion can be modelled as [92]:

$$y_{ik} = x_{ik} \cdot h_{ik} \cdot \exp(j\Phi_i) + n_{ik}, \tag{16}$$

for k_{th} subcarrier and i_{th} OFDM symbol [93]. Here y_{ik} and x_{ik} are the received and

transmitted data respectively, h_{ik} represents the channel distortion, Φ_i is the common phase rotation, and n_{ik} is the noise. It is clear that, noise is different for different OFDM symbols and different subcarriers; the common phase rotation, as has indicated by the name, is common for all subcarriers in an OFDM symbol but different for different OFDM symbols [56]. However, this assumption is valid only when the IFFT/FFT size is small and laser linewidth is small as well. The small laser linewidth effect is discussed in Section 4.3.3.

In this work, channel distortion are compensated or mitigated before pilot-aided CPE: attenuation compensated by EDFA inside fiber loops; CD compensated by overlap-and-save method; PMD mitigated by 1-tap equalization, and non-linear effects limited by controlling fiber launch power. Therefore, considering all channel distortion is fully compensated, Equation 3 can be simplified as:

$$y_{ik} = x_{ik} \cdot \exp(j\Phi_i) + n_{ik,} \tag{17}$$

As long as Φ_i is known, the transmitted data can be recovered as:

$$\hat{x}_{ik} = y_{ik} \cdot \exp(-j\Phi_i), \tag{18}$$

where $\hat{x}_{ik}$ represents the recovered data.

The common phase rotation can be obtained by calculating the phase difference between received and transmitted pilots. This difference is then averaged over an OFDM symbol:

$$\Phi_i = \frac{1}{N_p} \cdot \sum_{k=1}^{N_p} \arg\left(\frac{y_{ik}}{x_{ik}}\right), \tag{19}$$

where N_p is the number of pilot subcarriers and arg $(\frac{y_{ik}}{x_{ik}})$ is the phase difference between received and transmitted pilots.

4.2. RF-pilot phase noise compensation simulation results

The performance of the system using the RF-pilot tone method is affected by different factors, such as the PSR and the drive power for the MZM. Such dependencies will be discussed in this section to achieve the lowest system BER. In this section, these parameters are studied with a back-to-back setup. However, the conclusions are still valid for long-haul transmission. The performance with long-haul fiber is presented in Section 4.3, along with the performance using pilot-aided CPE method.

4.2.1. Selection of the number of subcarriers for data

Systems using OFDM use zero padding to combat aliasing. It is important to know the number of zero padding subcarriers required for maintaining an acceptable system BER, since subcarriers for zero padding consumes useful bandwidth.

Figure 21 shows the system BER performance with various number of data subcarriers. The FFT size is this figure is 128. The number of subcarriers for data is varied from 64 to 122. 64 data subcarriers result an oversampling rate of two; 122 is the maximum number

of data subcarriers in this system, since the remaining six subcarriers are reserved for the RF-pilot tone and RF-pilot's guard

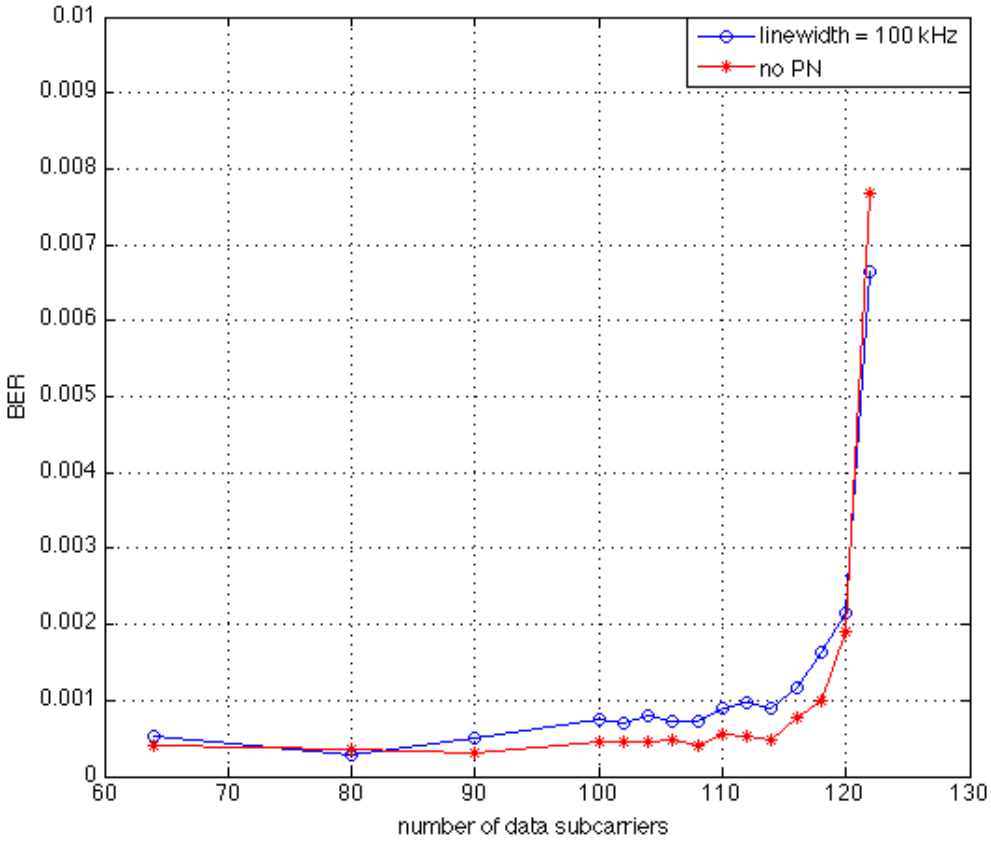

Figure 21 BER vs. Number of data subcarriers.

band. It can be seen that the system BER remains almost constant when the number of data subcarriers increases from 64 to 100, meaning that the number of zero padding is sufficient to combat aliasing; the system BER increases when the number of data subcarriers continues to increase. System BER shows severe degradation when the

number of data subcarriers is larger than 120. As is discussed in Section 4.1.1, the system with a 128-point FFT uses 100 subcarriers for data, maintaining an acceptable system BER without wasting useful bandwidth; also, it gives certain flexibility of the system when optical components changes or channel condition changes.

4.2.2. Impact of Pilot-to-Signal Ratio (PSR)

Here, the impact of the power ratio of RF-pilot and OFDM signal on the BER performance of the CO-OFDM system is discussed.

The PSR is defined as [89]:

$$PSR[dB] = 10\ log_{10}\left(\frac{P_{RF}}{P_{OFDM}}\right), \tag{20}$$

where P_{RF} is the electrical power of the RF-pilot and P_{OFDM} is the electrical power of the baseband OFDM signal.

The optimum PSR which gives the lowest BER performance depends on the laser linewidth [89] . To investigate the effect of the PSR on the system performance, we used a typical linewidth of 100 kHz for both the transmitter laser and LO. Figure 22 shows the variation of the BER with the PSR for various OSNRs and for an optical back-to-back configuration. For low values of PSR, the RF-pilot power may not be sufficient to

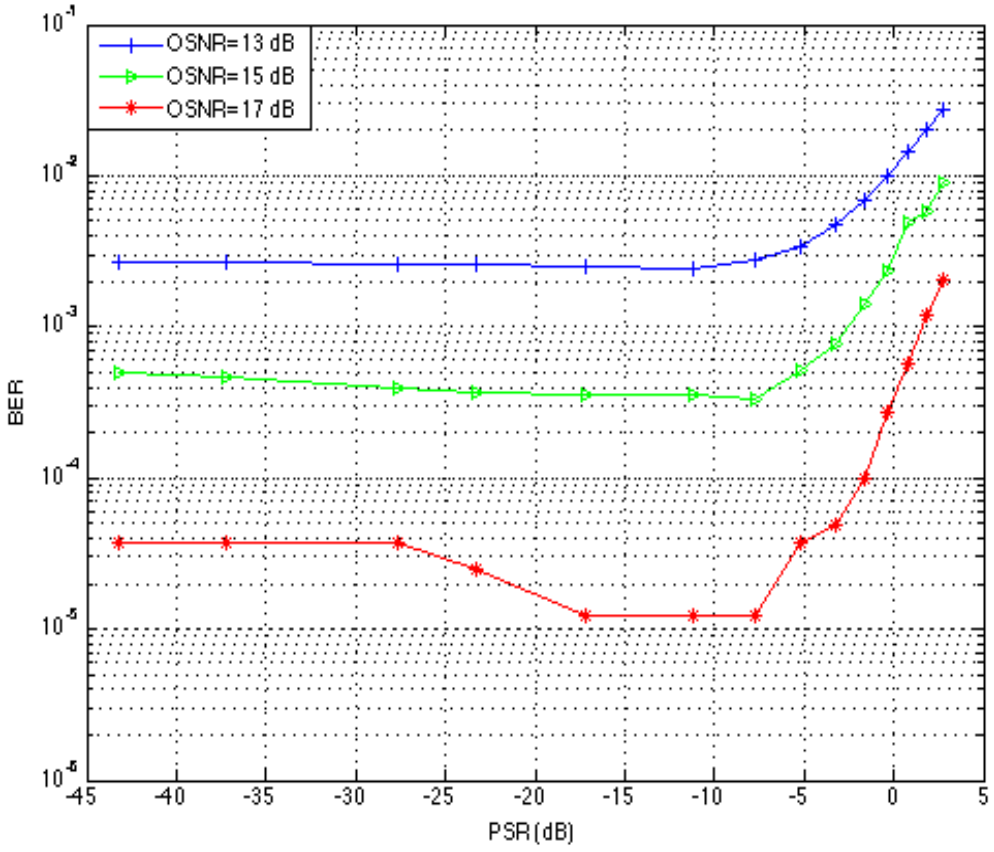

Figure 22 BER vs. PSR with various OSNRs.

compensate for the phase noise, while for higher PSRs, the OSNR of the OFDM signal becomes too low [94] . For example, for an OSNR of 17 dB, the BER improves slightly when the PSR is increased. When the PSR equals to -7.69 dB, the system has the lowest BER, and further increase in the PSR results in the degradation of the BER.

However, it can be observed from Figure 22 that in all cases, even when the PSR is as low as -44 dB, the BER is still in an acceptable range, considering the fact that no coding

is applied. The reason behind this is related to the extinction ratio of the Mach-Zehnder employed in the system. In this case, the extinction ratio of the MZMs is 20 dB. It is common value for a modulator used in a long-haul optical communication system. Its impact is elaborated in Section 4.2.3.

4.2.3. Impact of MZM extinction ratio

When choosing a modulator for a particular system, extinction ratio is an important parameter to consider, since it describes the content strength of the signal that the transmitter puts on the fiber [95]. MZM extinction ratio is defined as the ratio between the output optical power corresponding to the maximum transmission value and the one corresponding to the minimum transmission value in decibels. Larger extinction value indicates a larger difference between logical “1” and logical “0”, which is more robust against noise; smaller extinction ratio indicates a smaller difference between logical “1” and logical “0”, which is less robust against noise. However, modulators with larger extinction ratios cost more. It is important to choose modulators with an extinction ratio large enough to combat noise and is within reasonable cost range. Also, the higher the MZM extinction ratio is, the smaller a carrier residue exists. The existence of residue carrier results in less power in signal, leading to a smaller OSNR. This degrades the system BER performance. However, when considering the employment of RF-pilot phase noise compensation, the carrier residue overlaps with the sharp impulse caused by the added DC for phase noise compensation, together to contribute to the compensation

procedure and improves the system BER performance.

Figure 23 shows the system BER against PSR with MZMs of various extinction ratios. The OSNR in this figure is 15 dB. The extinction ratio is varied from 100 dB to 10 dB, representing modulator with an ideal extinction ratio and a more cost-efficient choice of modulator.

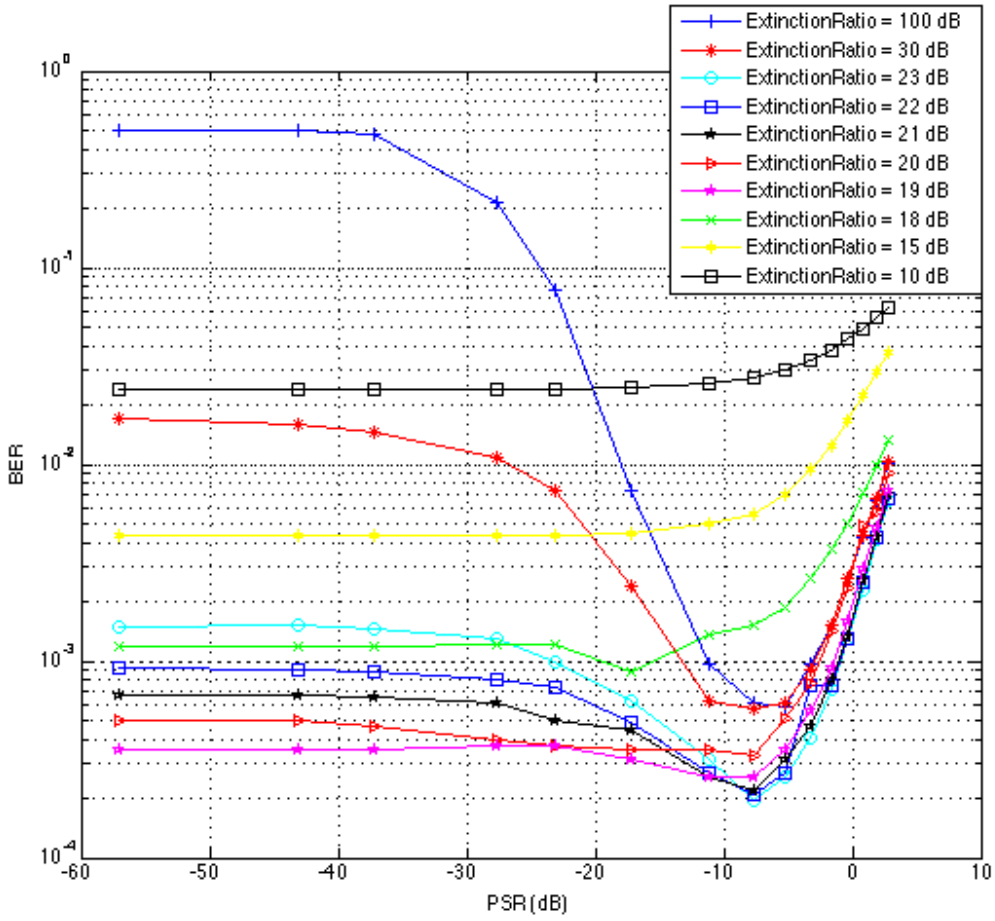

Figure 23 BER vs. PSR with various MZM extinction ratios.

Several interesting observations are made below pertaining to Figure 23:

First, from the discussion in 4.2.2, it is clear that, a theoretical optimum PSR exists. PSR higher than the optimum results in degradation in the system BER, and so does PSR lower than the optimum. However, in Figure 23, when the PSR decreases after ~37 dB, for any extinction ratio considered here, the system BER remains constant.

That is because even with an almost ideal extinction ratio, the carrier residue cannot be suppressed completely. The PSR is too small compared to the residue carrier. Phase noise compensation is mainly relying on the residual carrier instead of the RF-pilot. In small PSR region (smaller than ~35 dB in all cases of extinction ratio), the system BER remains constant. The reason behind that is for a certain extinction ratio, the suppressed residue carrier is fixed.

Second, the smaller the extinction ratio is, the larger the constant BER region is. The reason behind this is that modulators with smaller extinction ratio are less sensitive to the PSR change, due to the higher residue carriers. For extinction ratios as low as 15 dB or 10 dB, the increasing of PSR can no longer cause the system BER to drop. It only causes the lower OSNR in the signal.

Third, when decreasing the extinction ratio from 100 dB to 10 dB, the system BER does not exhibit a consistent trend. When decreasing the extinction ratio from 100 dB to 20 dB, the system BER decreases at a given PSR; when continuing decreases the extinction ratio

to 10 dB, the system BER increases at a given PSR.

When the extinction ratio is relatively high (20 dB and above), phase noise is the major impairment. Smaller extinction ratio results in a larger residue carrier. The residue carrier has more contribution than degradation to the system BER. When the extinction ratio is relatively low, the reduced OSNR caused by the low extinction ratio is the major impairment. The BER improvement from the improved phase noise compensation due to a larger residual carrier is significantly smaller than the degradation caused by the low OSNR in the signal. Hence the lack of consistency in BER trend.

The simulation results in Figure 24 confirm the third point. It shows the system BER against the transmission distance of fiber with various extinction ratios with optimum PSRs and without phase noise compensation. All curves show an increased BER when increasing the transmission distance, which is expected. The blue curves show the cases with an optimum PSR and without phase noise compensation at an extinction ratio of 15 dB. The gap between these two curves is small; the green curves show the cases with an optimum PSR and without phase noise compensation at an extinction ratio of 20 dB. The improvement in BER is more prominent when employing phase noise compensation with an optimum PSR; the red curves show the cases with an optimum PSR and without phase noise compensation at an extinction ratio of 30 dB. The gap between the curves with and without using phase noise compensation is huge. This confirms that when the extinction ratio is relatively low, the degradation in OSNR caused by the residue carrier is a major

impairment. Whether or not compensation exists, phase noise shows little difference in system BER. Phase noise is relatively low in both cases. When the extinction ratio is relatively high, the degradation in OSNR caused by the residue carrier is considerably small compared with the distortion caused by phase noise. That is the reason behind the huge gap between using and not using phase noise compensation. The cases with an extinction ratio of 20 dB are in between those extreme cases, and hence the medium gap.

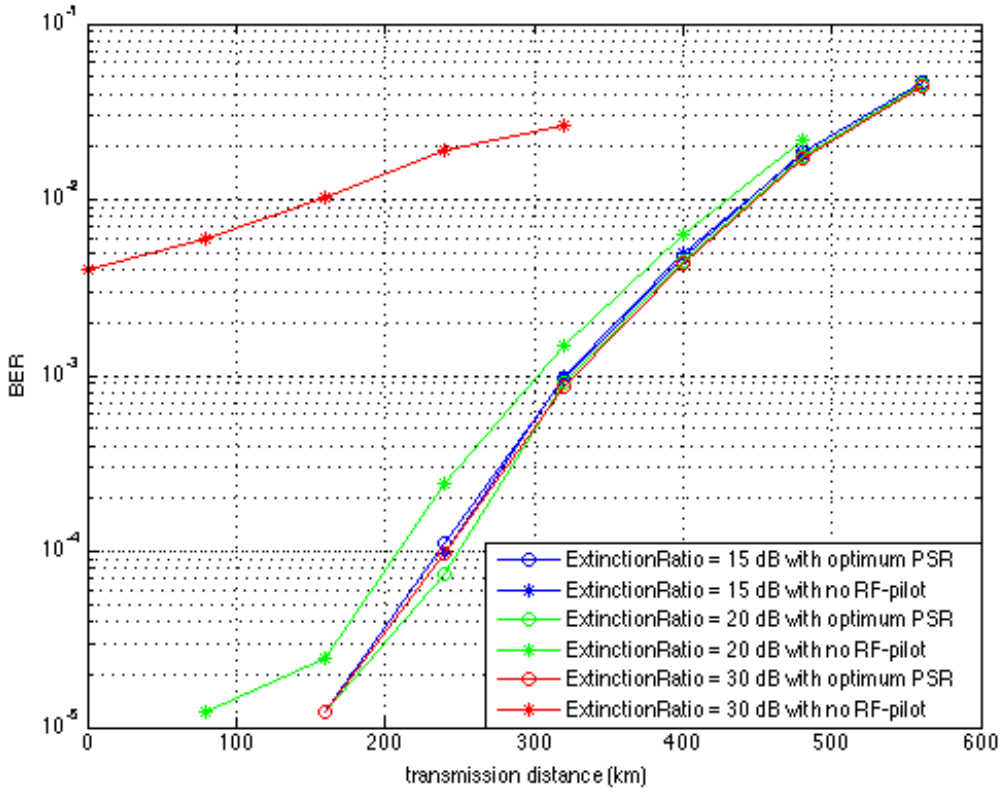

Figure 24 BER vs. transmission distance without RF-pilot.

The simulation results presented in later section are using MZMs with an extinction ratio

of 20 dB. It is a reasonable choice, considering the cost, its impact on signal OSNR, and its contribution to RF-pilot phase noise compensation.

4.2.4. Impact of MZM drive power

The level of the drive power to the MZMs also influences the system performance.

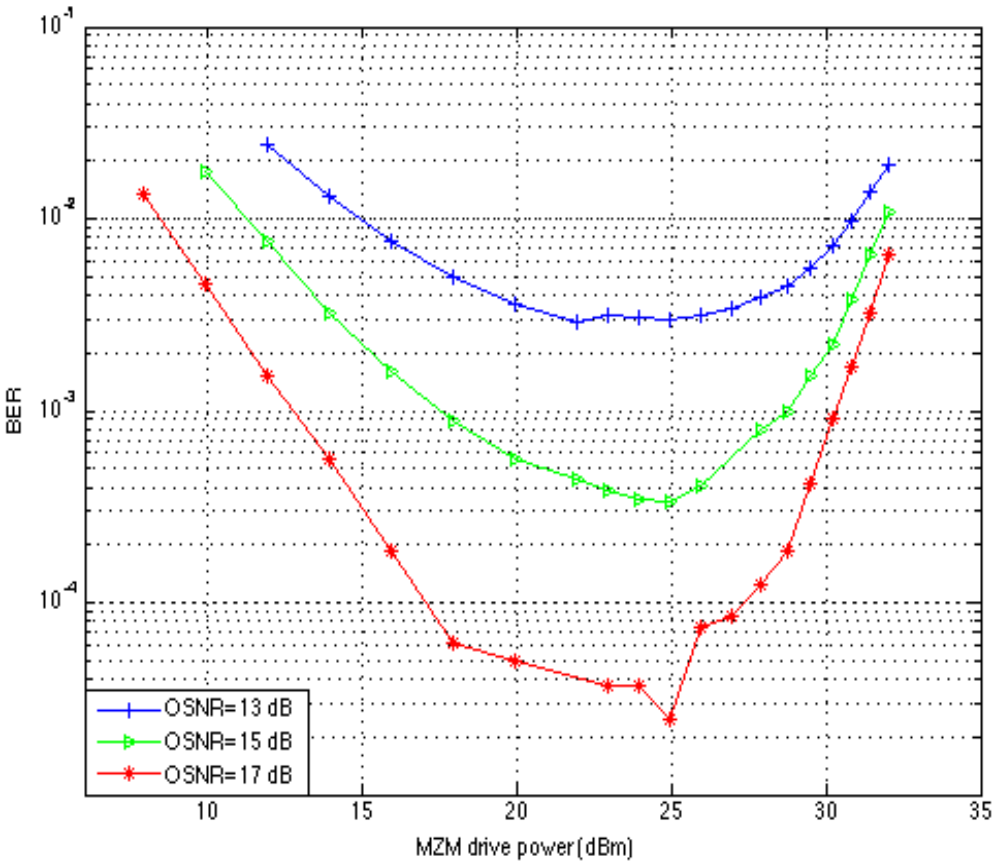

Figure 25 BER vs. MZM drive power.

As can be seen from Figure 25, the BER improves as the MZM drive power increases

from around 10 dBm up to an inflection point (drive power = 25 dBm in this case), beyond which it degrades. The trend is the same for various OSNRs.

This can be explained as follows: at low drive powers, the electrical SNR of the OFDM signal is low, which results in a poor BER. Increasing the drive power results in a corresponding increase in the electrical SNR and consequently, in reduced BER. On the other hand, at higher drive powers, the MZM nonlinear distortions set in, resulting in BER degradation.

4.2.5. Laser linewidth tolerance

Figure 26 shows the BER versus OSNR for various laser linewidths ranging from 0 to 1 MHz. As can be seen, for low values of OSNR, where the Gaussian white noise is the major distortion source, the performance remains almost the same for the different laser linewidths. However, at larger OSNRs, where the phase noise becomes the major impairment, an OSNR penalty of ~ 0.5 dB at a BER of 1×10^{-3} is observed when the laser linewidth is selected as 1 MHz. These results illustrate the effectiveness of the RF-pilot method for phase noise compensation.

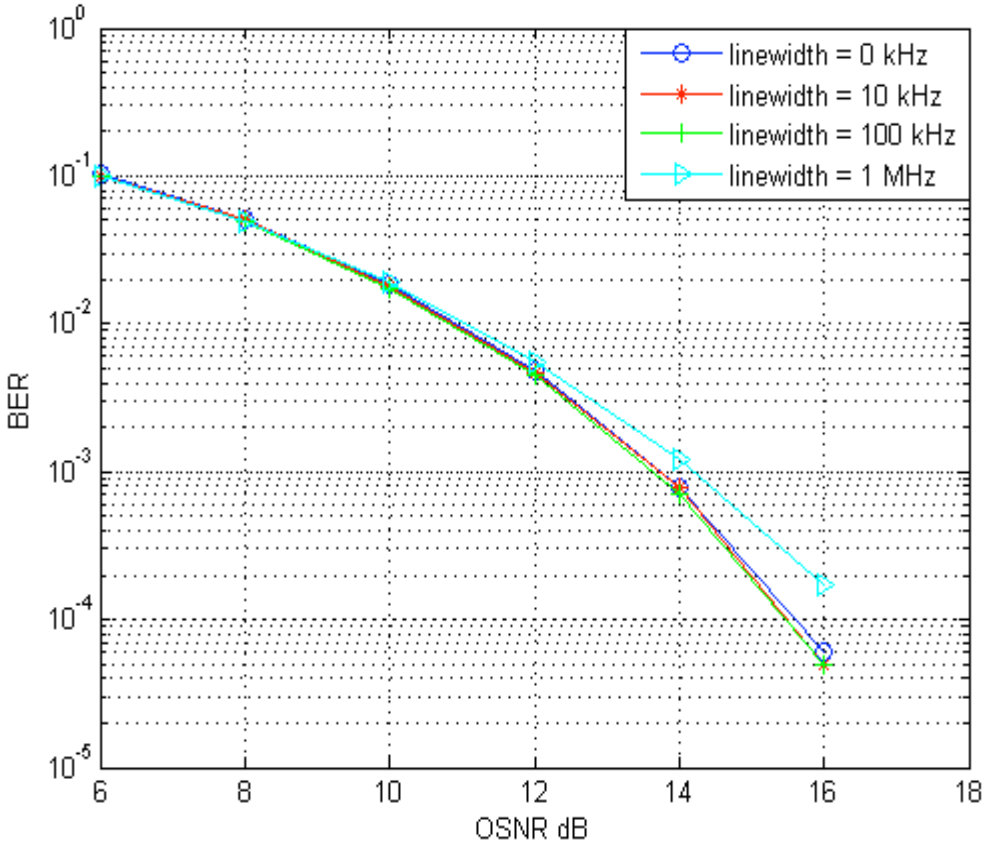

Figure 26 BER vs. OSNR with different linewidths.

4.3. Comparison between RF-pilot and pilot-aided CPE methods

In this section, the effectiveness and system overhead of the pilot-aided CPE compensation method and RF-pilot phase noise compensation method are compared. The system simulation set up is the same for both methods. The number of subcarriers reserved for the guard band for RF-pilot in the RF-pilot method is the same as the number of pilots when implementing the pilot-aided CPE method. In the latter case, the pilot

subcarriers are evenly spaced among the data subcarriers.

The modulation format is 4-QAM and FFT size is 128. The oversampling rate in this section is two (64 out of 128 subcarriers are used for data). A total number of 800 km SSMF is used. The SSMF parameters are: an effective area of $80\times10^{-12}\ m^2$, an attenuation of 0.2 dB/km, a dispersion (CD) of 16 ps/nm/km, and non-linear coefficient of $2.6\times10^{-20}\ s^2/W$. Attenuation is compensated by an amplifier with 16 dB gain and a noise figure of 4 dB within each fiber loop of 80 km. A frequency-domain equalizer using the overlap-add method [82] is utilized at the receiver side for CD compensation.

4.3.1. BER vs. number of subcarriers for phase noise compensation

It is important to know the minimum required number of subcarriers for phase noise compensation for both methods, since they consume useful bandwidth. Figure 27 shows the variation of the BER with the number of carriers reserved for pilots (pilot-aided CPE method) or number of carriers reserved for the guard band for RF-pilot (RF-pilot method) with 20 kHz laser linewidth. It can be seen that, for pilot-aided CPE method, with increase in the number of pilot subcarriers, the system BER decreases up to a point and then remains almost constant; for RF-pilot method, when the number of subcarriers reserved for the guard band for RF-pilots increases, the system BER shows a sharp decrease and then shows a trend to remain constant. The lowest achievable system BER is lower for RF-pilot method, although more subcarriers are required to achieve it.

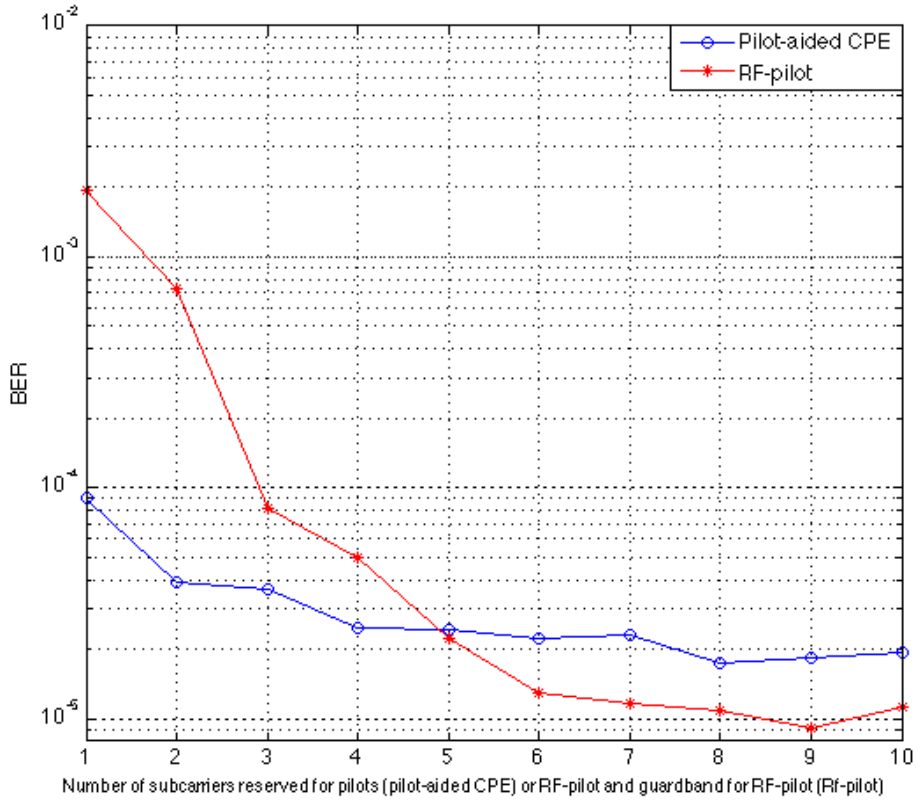

Figure 27 BER vs. number of subcarriers for pilots (pilot-aided CPE) or for the guard band for RF-pilot with a 20 kHz laser linewidth.

However, when the laser linewidth increases up to 100 kHz, as is shown in Figure 28, the trend for both methods remain the same, but the system BER using pilot-aided CPE method shows only a small decrease when increasing the pilot subcarrier numbers. The lowest achievable system BER for RF-pilot method ($\sim 1\times10^{-5}$) is much lower than that of pilot-aided CPE method ($\sim 2\times10^{-4}$), at the cost of only a few more subcarriers. For pilot-aided CPE method, four pilot subcarriers are sufficient for phase noise

compensation with a laser linewidth up to 100 kHz; for RF-pilot method, eight subcarriers for the guard band for RF-pilot are sufficient to achieve a desirable system BER.

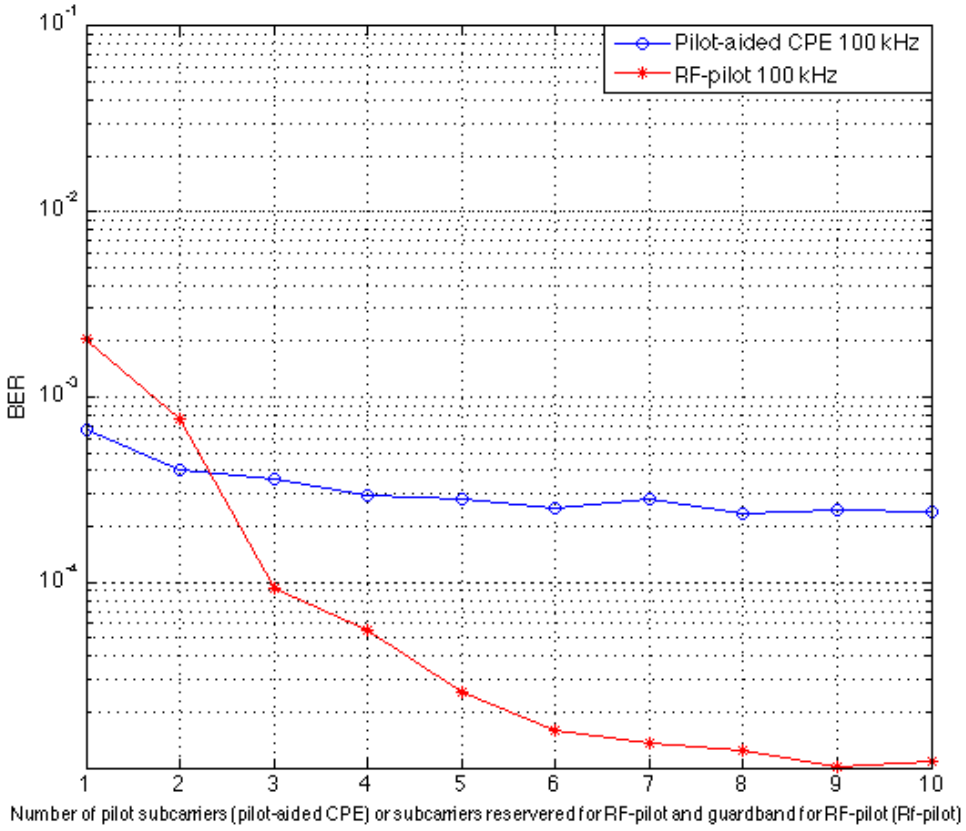

Figure 28 BER vs. number of subcarriers for pilots (pilot-aided CPE) or for the guard band for RF-pilot with a 100 kHz laser linewidth.

It can be concluded that the RF-pilot method achieves a lower BER at the cost of a few more subcarriers for phase noise compensation, when compared with the pilot-aided CPE method. Also, it can be predicted that, when the laser linewidth is increased even further,

RF-pilot method will show an even more superior BER performance.

4.3.2. BER vs. OSNR

Considering all the discussions above, including the necessary overhead for phase noise compensation and preferred system BER performance, it is reasonable to use four pilot subcarriers for pilot-aided CPE methods and eight subcarriers for the guard band for RF-pilot, since the system BER improves little despite further increasing the number of pilot subcarriers and so is the system BER of RF-pilot method.

Both compensation methods in Figure 29 use 64 null subcarriers out of 128 to combat aliasing. In this setup, pilot-aided CPE has 60 data subcarriers and RF-pilot method has 56 data subcarriers. Both methods have an oversampling rate of slightly higher than two. Figure 29 shows the system BER against OSNR for both phase noise compensation methods with this parameter setup.

It is clear that the system BER improves as the OSNR increases in both cases of phase noise compensation methods. RF-pilot compensation method shows a better BER performance at any given OSNR. At a given BER, 2×10^{-2} for instance, the required OSNR for pilot-aided CPE method is ~ 1.3 dB larger than the required OSNR for RF-pilot method; at the BER of 3×10^{-3}, pilot-aided CPE requires an OSNR 2 dB larger than what is required by RF-pilot. With the increase of the OSNR, the superiority of the RF-pilot is more prominent.

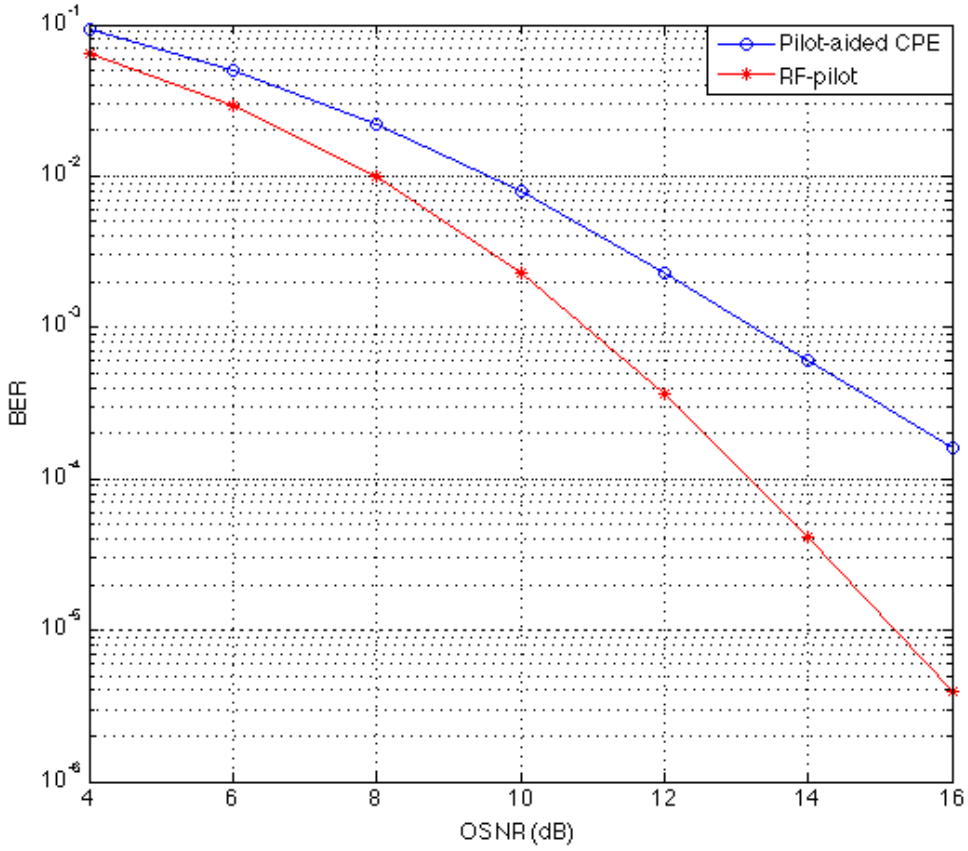

Figure 29 BER vs. OSNR for both phase noise compensation methods with same number of subcarriers for combating aliasing.

Instead of keeping same number of subcarriers to combat aliasing, Figure 30 shows the results when the number of data subcarriers is the same (64 out of 128) for both compensation methods, and the number of subcarriers for phase noise compensation and to combat aliasing combined together is 64. In this setup, the overall overhead for both compensation methods is the same. The oversampling rate for both methods is two. Pilot-aided CPE method still has four subcarriers for phase noise compensation, but the number

of null subcarriers for combating aliasing is 60; RF-pilot method still has eight subcarriers for phase noise compensation, but the number of null subcarriers to combat aliasing is 56.

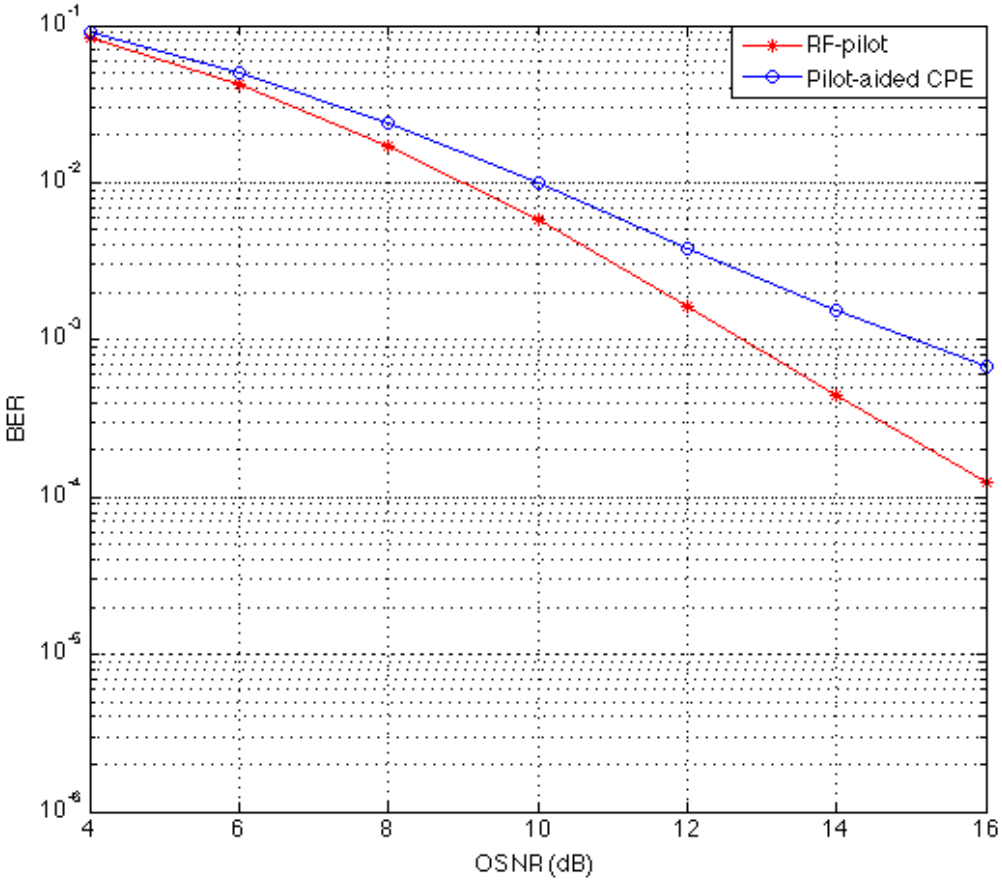

Figure 30 BER vs. OSNR for both phase noise compensation methods with same number of data subcarriers.

As can be seen from Figure 30, the trend of system BER performances with various OSNRs for both methods is the same. The trend is also similar to that of Figure 29. RF-pilot method still has a better performance regarding system BER. However, the BER is

degraded in both cases. The reason behind this change is the change in the number of null subcarriers for aliasing. The number of null subcarriers is smaller compared to that of Figure 29.

4.3.3. OSNR penalty vs. linewidth

In this section, further comparisons between pilot-aided CPE method and RF-pilot method are performed. Linewidth in this section is selected as 100 kHz. Figure 31 and Figure 32 show OSNR penalty vs. linewidth at BER of 2×10^{-2} and 3×10^{-3} respectively. OSNR at a certain BER at a certain linewidth here means the OSNR difference between the OSNR required to reach this BER without any phase noise and the OSNR required to reach the same BER with a laser with a certain linewidth.

As can be seen from Figure 31, RF-pilot method clearly has a larger tolerance to linewidth than pilot-aided CPE method: at any given OSNR penalty, RF-pilot method tolerates a much larger linewidth. For instance, at an OSNR penalty of ~ 3 dB, pilot-aided CPE has a linewidth of 200 kHz, and RF-pilot has a linewidth as large as 10 MHz. Figure 32 shows the same comparison between those two methods at a different BER. The trend and conclusion still stand.

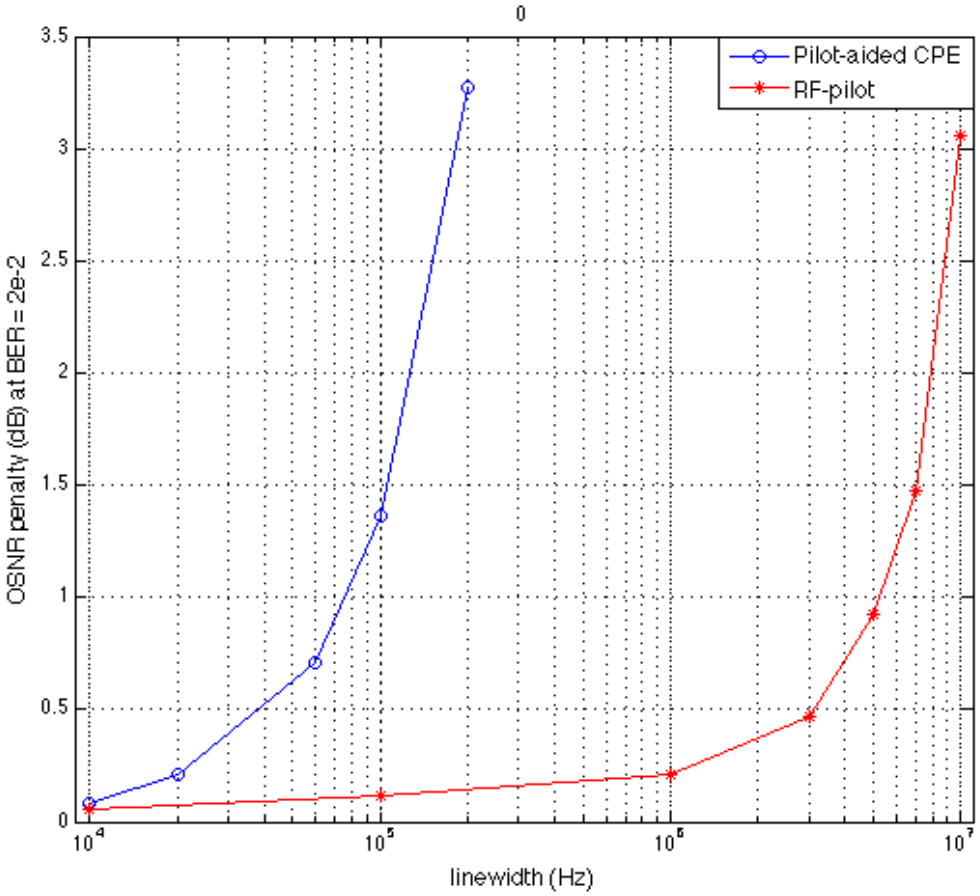

Figure 31 OSNR penalty at the BER of 2×10^{-2} vs. linewidth.

4.3.1. Overall comparison

From the results shown in the figures, it is clear that the RF-pilot method can effectively compensate for the phase noise at a cost of a slightly higher overhead, yet achieving a much better BER when compared with the conventional pilot-aided CPE method. RF-pilot method has a larger computational complexity. However, the RF-pilot method has a

significantly larger tolerance for linewidth.

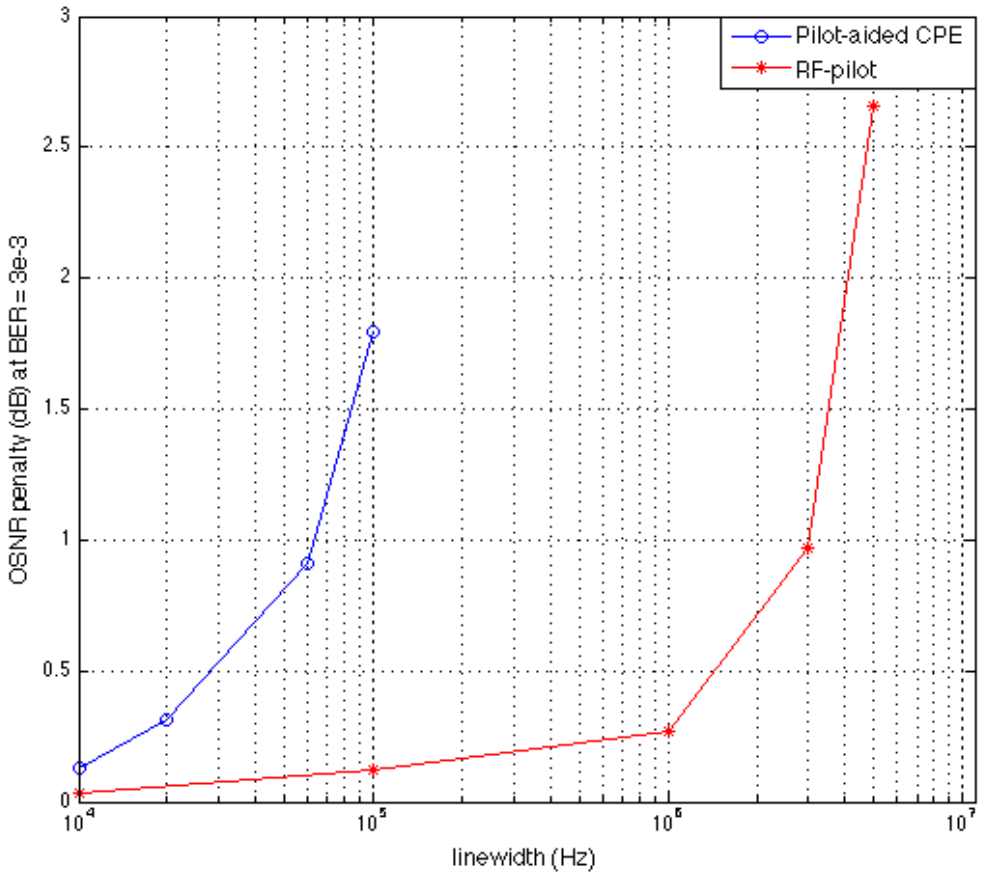

Figure 32 OSNR penalty at the BER of 3×10^{-3} vs. linewidth.

4.4. Chapter summary

In this chapter, the principles of two phase noise compensation methods are introduced and studied in detail: RF-pilot phase noise compensation method and pilot-aided CPE method. Various elements that affect the overall system performance are explored:

number of subcarriers allocated for the guard band for RF-pilot, PSR, MZM extinction ratio, and MZM drive power for RF-pilot method. Also, a detailed comparison including overhead, BER performance, and linewidth tolerance is performed for these two phase noise compensation. It can be concluded that RF-pilot method can reach a better BER performance at the cost of a slightly larger overhead (allocated subcarriers for phase noise compensation) and has a larger linewidth tolerance.

Chapter 5 Conclusions

In this thesis, DSP algorithms for major system impairment for long-haul CO-OFDM communication systems are studied, focusing on phase noise compensation. These algorithms mitigate system impairments. CD effects are compensated using overlap and save method; PMD effects are mitigated by 1-tap equalization and careful selection of training symbols; and, fiber non-linear effects are controlled by limiting fiber launch power. As for phase noise compensation, a comparative analysis is provided between RF-pilot method and pilot-aided CPE method.

In the investigation of the phase noise compensation, it has been found that many factors affect the performance of systems using RF-pilot: number of data subcarriers, PSR, MZM extinction ratio, MZM drive power. Some of the factors contradict each other and only a careful and systematic selection of parameters helps to obtain a preferred system BER with reasonable system cost. It has also been found out that RF-pilot method can reach a better system BER and a larger laser linewidth tolerance than pilot-aided CPE method. However, it is at the cost of a higher system complexity and slightly larger overhead in regard of the number of subcarriers reserved for phase noise compensation.

This thesis presents successful simulation of a CO-OFDM system with an optical fiber link with 800 km, and included compensation for CD, PMD effects, limiting the fiber

non-linear effects, and effective mitigation the laser phase noise. The systems in this work can obtain a BER of 10^{-5} at an OSNR of 15 dB at a data rate of 64 Gbit/s. The results of this work can be easily extended to WDM systems, thus facilitating ultrahigh data rates, and thus meeting the objective of the OmOptics Project.

- **Suggested future work**

Since phase noise is indeed a problem for coherent optical communication systems, it will be interesting to upgrade existing algorithms and explore new schemes for phase noise estimation and compensation. In the past few years, more research has been done to further improve the performance for phase noise compensation, such as combining RF-pilot and pilot-aided CPE phase noise compensation, using constant pilot frequencies and linear interpolation to estimate phase noise. It will also be a good direction to further explore the RF-pilot tone scheme for other system impairments, such as synchronization and combating nonlinearities. Also, PAPR is a major problem for systems employ OFDM. Using RF-pilot helps relieve the PAPR impact. It is worth to explore how much this schemes helps reducing PAPR and what other adaptations of the scheme can be developed to improve OFDM systems' performance.

References

[1] M. Arumugam, “Optical fiber communication - An overview,” *Pramana*, vol. 57, no. 5–6, pp. 849–869, Nov. 2001.

[2] R. Ramaswami, “Optical fiber communication: from transmission to networking,” *IEEE Commun. Mag.*, vol. 40, no. 5, pp. 138–147, May 2002.

[3] G. Agrawal, *Fiber-optic communication systems*, Hoboken, N.J: Wiley, vol. 6., 2002.

[4] B.E. Saleh, and M.C. Teich, *Fundamentals of Photonics*, Toronto: Wiley, vol. 5., 1991.

[5] K.C. Kao and G.A. Hockham, “Dielectric-fibre surface waveguides for optical frequencies,” *Proc. Inst. Electr. Eng.*, vol. 113, no. 7, p. 1151, Jul. 1966.

[6] R. Ramaswami, G.H. Sasaki, K.N. Sivarajan, *Optical Network*: *A practical perspective*, Burlington, Mass: Morgan Kaufmann Publishers, 3rd ed., March. 2006.

[7] R. Ramaswami, “Optical Fiber Communication: from transmission to networking,” *IEEE Commun. Mag.*, no. May, pp. 138–147, 2002.

[8] H.J.R. Dutton, “Understanding Optical Communications,” *Int. Tech. Support Organ.*, vol. 1, pp. 1–638, 1998.

[9] K. Kikuchi, *Coherent Optical Communications: Historical Perspectives and Future Directions*, Berlin, Heidelberg: Springer Berlin Heidelberg, vol 6., 2010.

[10] R. Noé, *Essentials of Modern Optical Fiber Communication*, Berlin, Heidelberg: Springer Berlin Heidelberg.

[11] International Telecommunications Union, “Optical Fibres, Cables and Systems,” pp. 144–147, 2010.

[12] P. Sharma, S. Pardeshi, R. Arora, and M. Singh, “A Review of the Development in the Field of Fiber Optic Communication Systems,” *Int. J. Emerg. Technol. Adv. Eng.*, vol. 3, no. 5, pp. 113–119, May 2013.

[13] G. Keiser, *Optical fiber communication*, 4th ed., New York, NY: McGraw-Hill, 2011.

[14] C. Xie, “Local Oscillator Phase Noise Induced Penalties in Optical Coherent Detection Systems Using Electronic Chromatic Dispersion Compensation,” *2009 Conf. Opt. Fiber Commun. - incudes post deadline Pap.*, no. 2, pp. 9–11, Mar. 2009.

[15] F. Grillot, C. Wang, N. Naderi, and J. Even, “Modulation properties of self-injected quantum-dot semiconductor diode lasers,” *IEEE J. Sel. Top. Quantum Electron.*, vol. 19, no. 4, Jan. 2013.

[16] B. Mukherjee, “WDM optical communication networks: progress and challenges,” *IEEE J. Sel. Areas Commun.*, vol. 18, no. 10, pp. 1810–1824, 2000.

[17] H. Takahashi, K. Takeshima, I. Morita, and H. Tanaka, “400-Gbit/s optical OFDM transmission over 80 km in 50-GHz frequency grid,” *Eur. Conf. Opt. Commun. ECOC*, vol. 1–2, pp. 19–21, Sep. 2010.

[18] X. Zhou, “Enabling technologies and challenges for transmission of 400 Gb/s signals in 50 GHz channel grid,” *Front. Optoelectron.*, vol. 6, no. 1, pp. 30–45, Nov. 2013.

[19] S. Gringeri, E.B. Basch, and T.J. Xia, “Technical considerations for supporting data rates beyond 100 Gb/s,” *IEEE Commun. Mag.*, vol. 50, Feb. 2012.

[20] T. Schenk, *RF imperfections in high-rate wireless systems: Impact and digital compensation,*1. Aufl. ed. Dordrecht: Springer Netherlands, 2008.

[21] J. Sakaguchi, Y. Awaji, N. Wada, A. Kanno, T. Kawanishi, T. Hayashi, T. Taru, T. Kobayashi, and M. Watanabe, “Space division multiplexed transmission of 109-Tb/s data signals using homogeneous seven-core fiber,” *J. Light. Technol.*, vol. 30, no. 4, pp. 658–665, Feb. 2012.

[22] K. Kikuchi, “Coherent Optical Communications-history, state-of-the-art technologies, and challenges for the future,” *Rev. Laser Eng.*, vol. 13, no. 6, pp. 460–466, 1985.

[23] E. Ip and J.M. Kahn, “Feedforward Carrier Recovery for Coherent Optical Communications,” *J. Light. Technol.*, vol. 25, no. 9, pp. 2675–2692, Sep. 2007.

[24] M. Kuschnerov, F.N. Hauske, K. Piyawanno, B. Spinnler, M.S. Alfiad, A. Napoli, and B. Lankl, “DSP for coherent single-carrier receivers,” *J. Light. Technol.*, vol. 27, no. 16, pp. 3614–3622, Aug. 2009.

[25] F. Herzel, S. Osmany, and J.C. Scheytt, “Analytical phase-noise modeling and charge pump optimization for fractional-N PLLs,” *IEEE Trans. Circuits Syst. I*

Regul. Pap., vol. 57, no. 8, pp. 1914–1924, Aug. 2010.

[26] D. Zibar, X. Yu, C. Peucheret, P. Jeppesen, and I.T. Monroy, “Digital coherent receiver for phase-modulated radio-over-fiber optical links,” *IEEE Photonics Technol. Lett.*, vol. 21, no. 3, pp. 155–157, Feb. 2009.

[27] S. Ristic, Bhardwaj, M.J. Rodwell, L. Coldren, and L. Johansson, “An Optical Phase-Locked Loop Photonic Integrated Circuit,” *J. Light. Technol.*, vol. 28, no. 4, pp. 526–538, Feb. 2010.

[28] K. Kikuchi, "Coherent transmission systems", *34th European Conference on Optical communications*, vol. 1, no. 39, pp. 21-25 Sep. 2008.

[29] L. G. Kazovsky and G. Kalogerakis, “Modern coherent optical communications,” *2006 Conf. Lasers Electro-Optics 2006 Quantum Electron. Laser Sci. Conf.*, vol. 1, pp. 11–12, Mar. 2006.

[30] R. Griffin, R.I. Johnstone, R.G. Walker, J. Hall, S.D. Wadsworth, K. Berry, C. Carter, M.J. Wale, J. Hughes, P. Jerram, and N.J. Parsons, “10 Gb/s optical differential quadrature phase shift key (DQPSK) transmission using GaAs/AlGaAs integration,” *Opt. Fiber Commun. Conf. Exhib.*, pp. 2–4, Mar. 2002.

[31] S. Tsukamoto, K. Katoh, and K. Kikuchi, “Coherent demodulation of optical multilevel phase-shift-keying signals using homodyne detection and digital signal processing,” *IEEE Photonics Technol. Lett.*, vol. 18, no. 10, pp. 1131–1133, May 2006.

[32] M.G. Taylor, “Coherent Detection Method Using DSP for Demodulation of Signal and Subsequent Equalization of Propagation Impairments,” *IEEE Photonics Technol. Lett.*, vol. 16, no. 2, pp. 674–676, May 2004.

[33] S. Tsukamoto, K. Katoh, and K. Kikuchi, “Unrepeated transmission of 20-Gb/s optical quadrature phase-shift-keying signal over 200-km standard single-mode fiber based on digital processing of homodyne-detected signal for group-velocity dispersion compensation,” *IEEE Photonics Technol. Lett.*, vol. 18, no. 9, pp. 1016–1018, May 2006.

[34] L. Tomba, “On the effect of wiener phase noise in OFDM systems,” *IEEE Trans. Commun.*, vol. 46, no. 5, pp. 580–583, May 1998.

[35] A. Demir, A. Mehrotra, and J. Roychowdhury, “Phase noise in oscillators: a unifying theory and numerical methods\nfor characterization,” *IEEE Trans. Circuits Syst. I Fundam. Theory Appl.*, vol. 47, no. 5, pp. 655–674, May 2000.

[36] M. Ahmed, M. Yamada, and M. Saito, "Numerical modeling of intensity and phase noise in semiconductor lasers," *IEEE J. Quantum Electron.*, vol. 37, no. 12, pp. 1600–1610, Dec. 2001.

[37] O. Llopis, P.H. Merrer, H. Brahimi, K. Saleh, and P. Lacroix, "Phase noise measurement of a narrow linewidth CW laser using delay line approaches," *Opt. Lett.*, vol. 36, pp. 2713–2715, Oct. 2011.

[38] N.Y. Voo, P. Horak, M. Ibsen, and W.H. Loh, "Linewidth and phase noise characteristics of DFB fibre lasers," pp. 2–9, Dec. 2004.

[39] E. Ip, A.P.T. Lau, D.J.F. Barros, and J.M. Kahn, "Coherent detection in optical fiber systems," *Opt. Express*, vol. 16, no. 2, pp. 753–791, Jan. 2008.

[40] Schäfter+Kirchhoff, "Fundamentals : Optical Modulators EOM Electro-Optical Phase Modulators with Fiber Optics Application.," Internet: http://www.sukhamburg.com/download/modulators_e.pdf

[41] B. Wedding, B. Franz, and B. Junginger, "10-Gb/s optical transmission up to 253 km via standard single-mode fiber using the method of dispersion-supported transmission," *J. Light. Technol.*, vol. 12, no. October, pp. 1720–1727, Oct. 1994.

[42] J. Armstrong, "OFDM for Optical Communications," *J. Light. Technol.*, vol. 27., no. 3., pp. 189-204, Feb.1, 2009.

[43] C. Browning, K. Shi, S. Latkowski, P. Anandarajah, F. Smyth, B. Cardiff, R. Phelan, and L.P. Barry, "Performance improvement of 10Gb/s direct modulation OFDM by optical injection using monolithically integrated discrete mode lasers," *2011 37th Eur. Conf. Exhib. Opt. Commun.*, vol. 19, no. 26, pp. 1–3, Dec. 2011.

[44] A. Peled and A. Ruiz, "Frequency domain data transmission using reduced computational complexity algorithms," *Icassp*, vol. 5, pp. 964–967, Apr. 1980.

[45] A.G. Armada, "Understanding the effects of phase noise in orthogonal frequency division multiplexing (OFDM)," *IEEE Trans. Broadcast.*, vol. 47, no. 2, pp. 153–159, Jun. 2001.

[46] A.S. Jensen, H. Hu, H. Ji, M. Pu, L.H. Frandsen, and L.K. Oxenløwe, *Impact of Nonlinearities on Fiber Optic Communications*, New York: Springer, vol. 7., 2011.

[47] M. Alard, M. Alard, R. Lassale, and R. Lassale, "Principles of modulation and channel coding for digital broadcasting for mobile receivers," *EBU Technical Review*, no. 224. pp. 168–190, 1987.

[48] I. Koffman and V. Roman, "Broadband wireless access solutions based on OFDM access in IEEE 802.16," *IEEE Commun. Mag.*, vol. 40, no. 4, pp. 96–103, Apr. 2002.

[49] B.I. Lembrikov, Y. Ben Ezra, M. Ran, M. Haridim, and G. Str, "High Spectral Efficiency Optical Transmission of OFDM Ultra-wideband Signals beyond 40 Gb/s," *ICTON*, vol.1, pp. 186-189, May 2006.

[50] X. Liu, Y. Qiao, and Y. Ji, "Inline dispersion compensation effect for 100Gb/s PDM-CO-OFDM long-haul transmission systems," *Proc. - 2010 2nd IEEE Int. Conf. Netw. Infrastruct. Digit. Content, IC-NIDC 2010*, pp. 897–901, Sep. 2010.

[51] A.J. Lowery, L. Du, and J. Armstrong, "Orthogonal Frequency Division Multiplexing for Adaptive Dispersion Compensation in Long Haul WDM Systems," *Optical Society of America*, p. 39, Mar. 2006.

[52] I.B. Djordjevic and B. Vasic, "Orthogonal frequency division multiplexing for high-speed optical transmission," *Opt. Express*, vol. 14, no. 9, pp. 3767–3775, May 2006.

[53] Q. Yang, A. Amin, and W. Shieh, *Optical OFDM Basics*, New York, NY: Springer New York, vol. 7., pp. 43-85, 2011.

[54] W. Shieh and I.B. Djordjevic, *OFDM for OPtical Communications*, 1st ed., Burlington, MA: Academic Press/Elsevier, 2010.

[55] S. L. Jansen and D. van den Borne, "SC341 OFDM for Optical Communications," *OFC/NFOEC*, pp. 1–74, Mar. 2013.

[56] X. Yi, W. Shieh, and Y. Ma, "Phase Noise Effects on High Spectral Efficiency Coherent Optical OFDM Transmission," *J. Light. Technol.*, vol. 26, no. 10, pp. 1309–1316, May 2008.

[57] W. Shieh, H. Bao, and Y. Tang, "Coherent optical OFDM: theory and design," *Opt. Express*, vol. 16, no. 2, pp. 841–859, Jan. 2008.

[58] B.J.C. Schmidt, A.J. Lowery, and J. Armstrong, "Experimental Demonstrations of 20 Gbit / s Direct-Detection Optical OFDM and 12 Gbit / s with a colorless transmitter," *Ratio*, pp. 20–22, Mar. 2007.

[59] W. Shieh, X. Yi, and Y. Tang, "Transmission experiment of multi- gigabit coherent optical OFDM systems over 1000 km SSMF fibre," *Electronic Letters*, vol. 43, no. 3, pp. 3–4, Feb. 2006.

[60] Z. Zalevsky, S. Ben-Yaish, E. Guetta, Y. Beiderman, and S. Gannot, “Optical realization of Viterbi decoder for communication network,” *Opt. Express*, vol. 15, no. 7, pp. 3635–3649, Apr. 2007.

[61] G. Colavolpe, S. Member, T. Foggi, E. Forestieri, and M. Secondini, “Impact of Phase Noise and Compensation Techniques in Coherent Optical Systems,” *J. Light. Technol.*, vol. 29, no. 18, pp. 2790–2800, Sep. 2011.

[62] K.F. Renk, *Basics of Laser Physics*, 2012 ed. Berlin, Heidelberg: Springer Berlin Heidelberg, 2012.

[63] Y. Atzmon and M. Nazarathy, “Laser phase noise in coherent and differential optical transmission revisited in the polar domain,” *J. Light. Technol.*, vol. 27, no. 1, pp. 19–29, Jan. 2009.

[64] V. Syrjälä, M. Valkama, N.N. Tchamov, and J. Rinne, “Phase noise modelling and mitigation techniques in OFDM communications systems,” *2009 Wirel. Telecommun. Symp*, pp. 1-7, May 2009.

[65] G. Agrawal, “Nonlinear fiber optics: its history and recent progress [invited],” *J. Optical Society of America*, vol. 28, no. 12, pp. 1–10, Nov. 2011.

[66] A. Pinto, "Optical Networks: A Practical Perspective," 2nd ed., J. *Opt. Netw*., vol. 1., pp. 219-220, 2002.

[67] R.J. Essiambre, G. Kramer, P.J. Winzer, G.J. Foschini, and B. Goebel, “Capacity Limits of Optical Fiber Networks,” *J. Light. Technol.*, vol. 28, no. 4, pp. 662–701, Feb. 2010.

[68] M.N. Chughtai, "Study of physical layer impairments in high speed optical networks," M.A. thesis, KTH School of Information and Communication Technology, Stockholm, Sweden, 2012.

[69] X. Yi, “Signal Processing Techniques for Optical Fiber Networks,” PhD. thesis, University of Melbourne, Australia, 2007.

[70] Q. Zhuge, M. Morsy-Osman, and D.V. Plant, “Analysis of dispersion-enhanced phase noise in CO-OFDM systems with RF-pilot phase compensation,” *Opt. Express*, vol. 19, no. 24, pp. 24030–6, Nov. 2011.

[71] C. Chen, Q. Zhuge, and D.V. Plant, “Zero-guard-interval coherent optical OFDM with overlapped frequency-domain CD and PMD equalization,” *Opt. Express*, vol. 19, no. 8, pp. 7451–7467, Apr. 2011.

[72] L. Thevenaz, V. de Coulon, and J. P. von der Weid, “Polarization-mode interferometry in birefringent single-mode fibers,” *Opt. Lett.*, vol. 12, no. 8, pp. 619-621, Aug. 1987.

[73] D. Chowdhury, “PMD induced system impairments in long-haul optical communication system,” *1999 IEEE LEOS*, vol. 1, pp. 147–148, 1999.

[74] S. Ten and M. Edwards, “An Introduction to the Fundamentals of PMD in Fibers,” p. White Paper WP5051, Jul. 2010.

[75] O. Solgaard, J. Park, J. B. Georges, P. K. Pepelijugoski, and K. Y. Lau, “Millimeter wave, multigigahertz optical modulation by feedforward phase noise compensation of a beat note generated by photomixing of two laser diodes,” *IEEE Photonics Technol. Lett.*, vol. 5, no. 5, pp. 574–577, May 1993.

[76] Z. Xiang and Y. Jianjun, “Recent Progress in High-speed and High Spectral Effi ciency Optical Transmission Technology,” Internet: www.chinacommunications.cn/fileup/PDF/2010-7-3-003.pdf, 2010.

[77] S.J. Savory, A.D. Stewart, S. Wood, G. Gavioli, M.G. Taylor, R.I. Killey, and P. Bayvel, “Digital equalisation of 40Gbit/s per wavelength transmission over 2480km of standard fibre without optical dispersion compensation,” *ECOC*, pp. 4–5, 2006.

[78] E.M. Ip and J.M. Kahn, “Fiber Impairment Compensation Using Coherent Detection and Digital Signal Processing,” *J. Light. Technol.*, vol. 28, pp. 502–519, Feb. 2010.

[79] G. Agrawal, “Nonlinear Fiber Optics and its Applications in Optical Signal Processing,” Internet: http://www.optics.rochester.edu/users/gpa/nlfo_1h.pdf, 2007.

[80] “VPItransmissionMaker^{TM}Optical Systems – Overview.” Internet: http://www.vpiphotonics.com/Tools/OpticalSystems/,Accessed: 12-May-2015.

[81] “VPItransmissionMaker/VPIcomponentMaker Simulation Guide.” VPItransmissionMaker^{TM}Optical Systems software help document, 2015.

[82] R. Kudo, T. Kobayashi, K. Ishihara, Y. Takatori, A. Sano, and Y. Miyamoto, “Coherent Optical Single Carrier Transmission Using Overlap Frequency Domain Equalization for Long-Haul Optical Systems,” *J. Light. Technol.*, vol. 27, no. 16, pp. 3721–3728, Aug. 2009.

[83] S. S. Haykin, *Adaptive filter theory*. Englewood Cliffs, NJ: Prentice Hall, 1991.

[84] G. Li, “Coherent Optical Communication,” *OSA/AOE*, pp. 2–4, 2008.

[85] T. Xu, G. Jacobsen, S. Popov, J. Li, E. Vanin, K. Wang, A. T. Friberg, and Y. Zhang, “Chromatic dispersion compensation in coherent transmission system using digital filters,” *Opt. Express*, vol. 18, no. 15, pp. 16243–16257, Jul. 2010.

[86] S. Deng, X. Yi, M. Deng, Z. Luo, Q. Yang, M. Luo, and K. Qiu, “Reduced-guard-interval OFDM using digital sub-band-demultiplexing,” *IEEE Photonics Technol. Lett.*, vol. 25, no. 22, pp. 2174–2177, Nov. 2013.

[87] “Algorithms for communications systems and their applications,” *Scitech Book News*, vol. 27, no. 1. Ringgold Inc, Portland, p. 161, 2003.

[88] D. Lowe and X. Huang, “Adaptive Overlap-Add Equalization for MB-OFDM Ultra-Wideband,” *ISCIT* , pp.644-648, Sep. 2006.

[89] S. L. Jansen, I. Morita, T. C. W. Schenk, and N. Takeda, “Coherent Optical 25 . 8-Gb / s OFDM Transmission Over 4160-km SSMF,” *Lightwave*, vol. 26, no. 1, pp. 6–15, Jan. 2008.

[90] S. Randel, S. Adhikari, and S. L. Jansen, “Analysis of RF-pilot-based phase noise compensation for coherent optical OFDM systems,” *IEEE Photonics Technol. Lett.*, vol. 22, no. 17, pp. 1288–1290, Sep. 2010.

[91] O. Omomukuyo, D. Chang, J. Zhu, O. Dobre, R. Venkatesan, T. Ngatched, and C. Rumbolt, “Joint timing and frequency synchronization based on weighted CAZAC sequences for reduced-guard-interval CO-OFDM systems,” *Opt. Express*, vol. 23, no. 5, p. 5777, Feb. 2015.

[92] X. Yi, W. Shieh, and Y. Tang, “Phase estimation for coherent optical OFDM,” *IEEE Photonics Technol. Lett.*, vol. 19, no. 12, pp. 919–921, Jun. 2007.

[93] X. Yi, W. Shieh, and Y. Tang, “Phase Estimation for Coherent Optical OFDM Transmission,” *COIN-ACOFT*, vol. 19, no. 12, pp. 919–921, Jun. 2007.

[94] S. L. Jansen, I. Morita, and H. Tanaka, “10-Gb / s OFDM with conventional DFB lasers,” *ECOC*, vol. 1, no. 2, pp. 16-20, Sep. 2007.

[95] A. Sheetal, A. K. Sharma, and R. S. Kaler, “Impact of extinction ratio of single arm sin2 LiNbO3 Mach-Zehnder modulator on the performance of 10 and 20 Gb/s NRZ optical communication system,” *Optik (Stuttg).*, vol. 120, no. 14, pp. 704–709, Feb. 2009.